



## A look back, part II: The drilling campaign of the Curiosity rover during the Mars Science Laboratory's second and third martian years

William Abbey<sup>\*</sup>, Robert Anderson, Luther W. Beegle, Gregory Peters, John Michael Morookian, Jeffrey Biesiadecki, Joseph Carsten, Curtis Collins, Kevin Davis, Ryan Kinnett, Douglas Klein, Stephen Kuhn, Cambria Logan, Mark Maimone, Joseph Melko, Avi Okon, Jason Reid, Matt Robinson, Jaime Singer, Vandii Verma, Ashwin R. Vasavada

*Jet Propulsion Laboratory, California Institute of Technology, 4800 Oak Grove Drive, Pasadena, CA 91109, United States of America*

### ARTICLE INFO

#### Keywords:

Mars  
Instrumentation  
Mars, surface  
Prebiotic environments

### ABSTRACT

The Mars Science Laboratory (MSL) rover, Curiosity, completed its second Martian year, 1337 sols (1374 Earth days), of operation on May 11, 2016, and its third Martian year, 2006 sols (2061 Earth days), of operation on March 28, 2018. During this time the rover successfully drilled twelve full depth drill holes into the Martian surface and analyzed the recovered material using onboard instruments, giving us new insights into the potential habitability and geologic diversity of ancient Mars. During the second Martian year, four holes were drilled into the mudstones of the Murray formation: 'Confidence Hills' (Sol 759), 'Mojave 2' (Sol 882), 'Telegraph Peak' (908) & 'Buckskin' (Sol 1060); while four more holes were drilled into the sandstones of the Stimson formation: 'Big Sky' (Sol 1119), 'Greenhorn' (Sol 1137), 'Lubango' (Sol 1320) & 'Okoruso' (Sol 1332). During the third Martian year, four additional holes were drilled into the Murray formation: 'Oudam' (Sol 1361), 'Marimba' (Sol 1422), 'Quela' (Sol 1464) & 'Sebina' (Sol 1495). In this paper, we will give a brief overview of the rover sampling hardware and nominal drilling protocols, followed by a discussion of how these protocols were refined and altered early during the course of Curiosity's second year on Mars. In addition, we will describe the 'Bonanza King' (Sol 724) drill campaign, the mission's first 'successful failure', and how it influenced these changes. We will also briefly discuss the events leading up to the drill feed fault on Sol 1536, which resulted in suspension of all drill activities for the remainder of the third Martian year. Finally, we will present scientific highlights obtained from each drill site utilizing MSL's onboard instrumentation (SAM & CheMin), results enabled by the drill's ability to excavate sample at depth and transfer it to these instruments.

### 1. Introduction

On August 6, 2012, the Mars Science Laboratory mission's rover, Curiosity, landed in Gale crater on Mars with the goal of gaining a better understanding of the past and present habitability of the planet (Grotzinger et al., 2012). The first autonomous drill designed by NASA capable of penetrating solid rock is attached to the robotic arm (Anderson et al., 2012). During the course of its first Martian year, 669 sols or Martian days (or 687 Earth days), three full depth drill holes were drilled into Aeolis Palus, the plain separating the northern rim of the crater from the foothills of the crater's central mound, Aeolis Mons ("Mount Sharp") (Abbey et al., 2019). The first two, John Klein (Sol 182) and Cumberland (Sol 279), were made in the mudstones of the

Yellowknife Bay formation. The third, Windjana (Sol 621), was made in the sandstones of the Kimberley formation. Analysis of the samples acquired at these sites led to the discovery that Gale crater may once have been habitable for Earth-like organisms (Grotzinger et al., 2014), the first in situ formation and surface exposure age determinations (Farley et al., 2014), and the first definitive detection of organics on the Martian surface (Freissinet et al., 2015). Curiosity completed its second Martian year of operation on May 11, 2016, and its third Martian year of operation on March 28, 2018, during which time it successfully drilled an additional twelve full depth drill holes on the planet's surface.

The primary purpose of the rover's drill is to acquire samples of powder from rock interiors for delivery to the SAM (Sample Analysis at Mars) and CheMin (Chemistry & Mineralogy) instruments onboard

<sup>\*</sup> Corresponding author.

E-mail address: [William.J.Abbey@jpl.nasa.gov](mailto:William.J.Abbey@jpl.nasa.gov) (W. Abbey).

<https://doi.org/10.1016/j.icarus.2020.113885>

Received 21 January 2020; Received in revised form 17 April 2020; Accepted 27 May 2020

Available online 2 June 2020

0019-1035/© 2020 Elsevier Inc. All rights reserved.

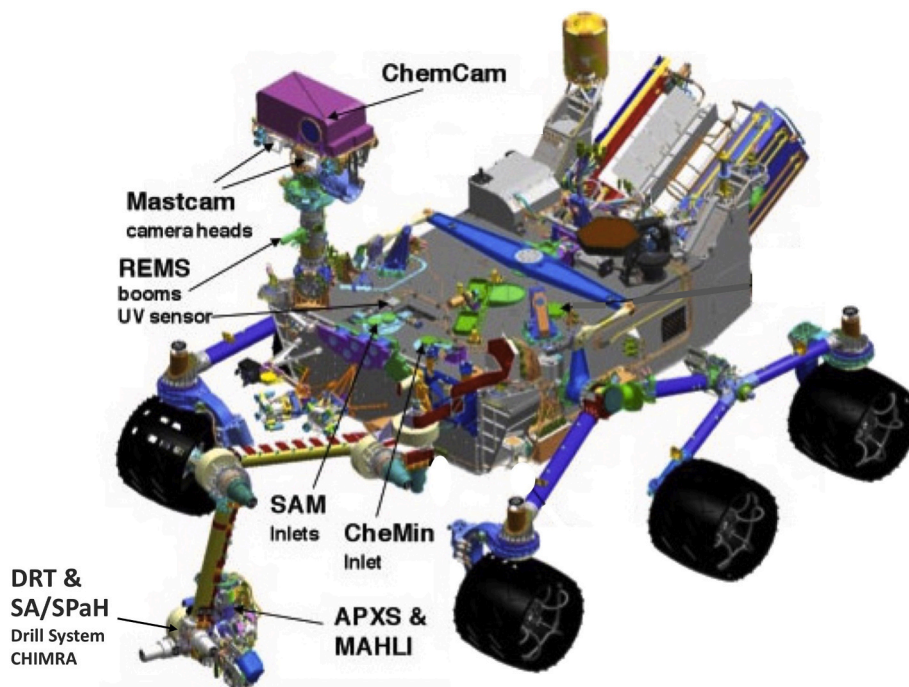


**Fig. 1.** Schematic image of rover showing location of tools and instruments referenced in this paper, including mast-mounted Mastcams and ChemCam and turret-mounted APXS, MAHLI, DRT and SA/SPaH systems. SAM and CheMin are onboard instruments housed within the body of the rover. The Rover Environmental Monitoring Station (REMS) is also shown. Rover is 2.9 m long by 2.7 m wide by 2.2 m in height.

Curiosity (Fig. 1). Together these two analytical laboratories analyze samples to help understand the formation and history of a sample including the past and present habitability of Mars. SAM is a combination mass spectrometer and gas chromatograph capable of detecting organic compounds and other (light) elements relevant to life. Additionally, it has a Tunable Laser Spectrometer (TLS) capable of detecting  $\text{CH}_4$ ,  $\text{CO}_2$ , and  $\text{H}_2\text{O}$ , including determination of isotopic ratios. CheMin uses X-ray diffraction to determine definitive mineralogy. The drill itself is part of the Sample Acquisition/Sample Processing and Handling (SA/SPaH) subsystem mounted on the end of the rover arm, along with a Dust Removal Tool (DRT), the Alpha-Particle X-ray Spectrometer (APXS), to determine elemental chemistry, and the Mars Hand Lens Imager (MAHLI), a high resolution color camera. Both APXS and MAHLI are used extensively by the team to better understand the nature of potential drill targets and whether or not they are safe for full depth drilling. In addition to the arm mounted instruments, drill target triage is also aided by mast-mounted cameras (Mastcams) and a mast-mounted Laser Induced Breakdown Spectroscopy (LIBS)-based instrument (ChemCam) capable of determining elemental chemistry from a standoff distance of up to 7 m. The total suite of instruments available on the rover is summarized more completely in Grotzinger et al. (2012).

## 2. Overview of nominal drilling protocol and SA/SPaH hardware

An overview of the SA/SPaH hardware, target assessment protocols, and drilling parameters have all been discussed in more detail elsewhere, but will be summarized here for the sake of convenience (Abbey et al., 2019; Anderson et al., 2012). This section describes drilling protocols and procedures that were utilized throughout the Prime Mission during the first Martian year and were considered ‘nominal’ by the start of the second Martian year. However, during the second Martian year, challenges arose that necessitated changes to these standard procedures, as well as the development of new protocols, in order to ensure the continued success of the mission. These improvements, and the events that led up to them, are documented in more detail in Sections 3 and 4.

Prior to drilling a new target, a target assessment analysis is

performed to ensure the safety of the flight hardware including the SA/SPaH, SAM and CheMin instruments. This ‘sample triage’ involves: 1) studying the local geology/chemistry of the site to better understand the nature of the sample, 2) assessing any potential engineering concerns involving target reachability, rover slip risks, stability of the rock being drilled, etc., and 3) determining if we have prior experience, either in our Earth-based testbed or on Mars itself, drilling the type of proposed target material in terms of the morphology, likely physical parameters, and likely mineralogy of the sample. In particular, the SA/SPaH subsystem requires that the sample ingested behave like a dry, fine-grained, granular powder; the system is not designed to handle wet or sticky samples, and even on a dry planet like Mars this is a potential problem as some minerals (e.g., Fe-sulfates) may deliquesce at high relative humidity inside of SA/SPaH or release bound water by drilling-induced heating. This may cause drill fines to become sticky and behave more like a paste than dry powder, potentially clogging the SA/SPaH passageways and sieves. In order to mitigate this problem, a test hole is created prior to full depth drilling. This test hole, or mini-drill hole, is operationally similar to a full depth drill hole and follows an almost identical procedure described below. In brief, a test hole begins with the Start Hole protocol, followed by a Hardness Test, before drilling a hole approximately 2 cm deep into the rock target. At this depth, the drill stops short of ingesting drilled material into the Drill Bit Assembly, giving the team an opportunity to examine the powdered drill tailings that have accumulated around the hole. Visual imaging from Mastcam and Navcam is used to determine if the particles behave like a dry

**Table 1**  
Percussion levels.

Level	Impact energy (J)	Impact velocity (m/s)	Impact force (N)
1	0.05	0.50	1500
2	0.20	1.00	3000
3	0.31	1.25	3750
4	0.45	1.50	4500
5	0.67	1.75	5200
6	0.80	2.00	6000

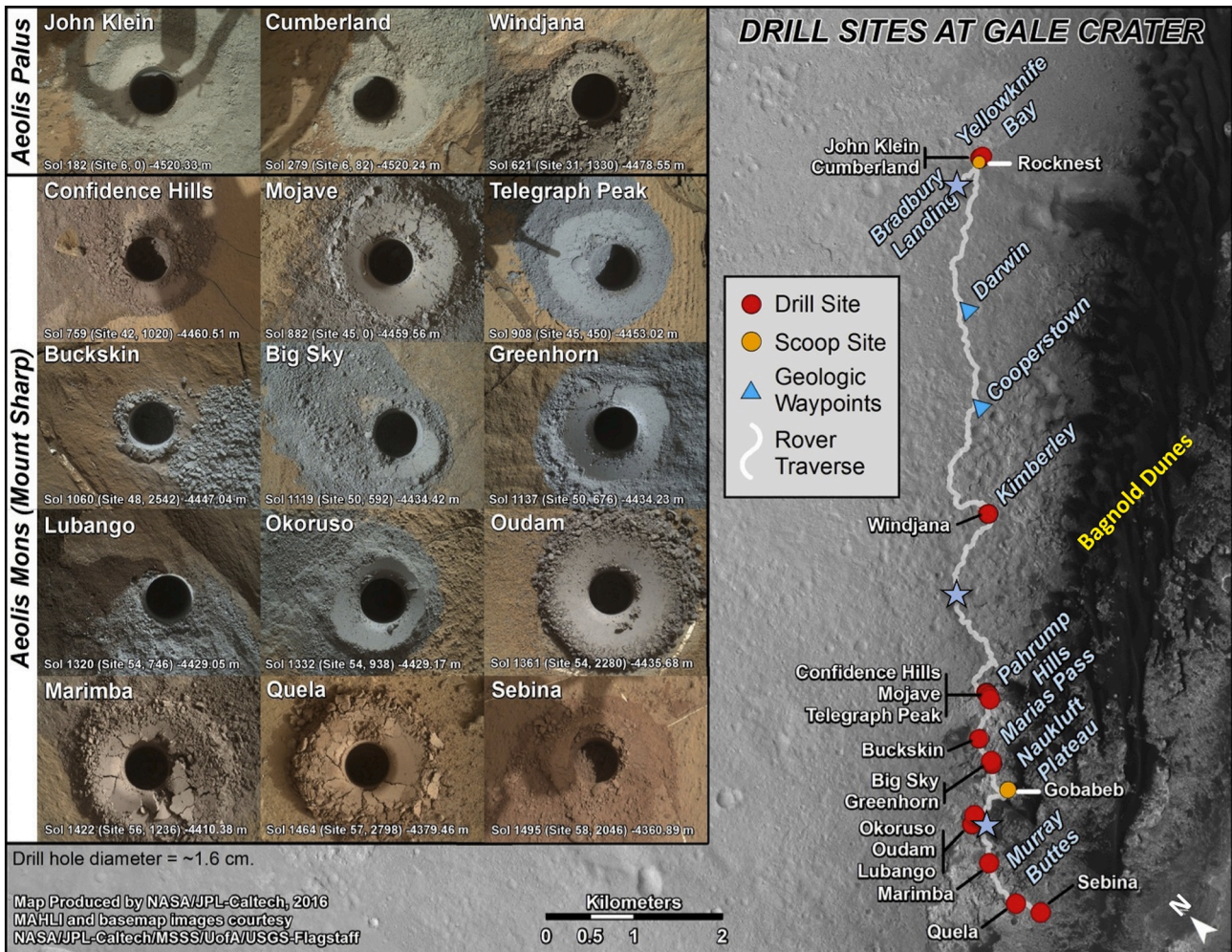


**Fig. 2.** HiRISE image showing the route (white line) driven by Curiosity through Sol 1495 during the third Martian year (modified after PIA21254). Blue stars represent the traverse from Bradbury Landing through Sol 669, the completion of the first Martian year, and Sol 1337, the completion of the second Martian year. Red circles indicate drill locations and yellow circles indicate scooping locations during this time period. Blue triangles represent geologic waypoints. (insets) MAHLI images of all full depth drill holes taken at a standoff of 10 cm with the exception of Sebina, which was taken at a standoff of 25 cm. Note first three full depth drill holes were created during the Prime Mission, but are included here for completeness. Drill holes are 1.6 cm in diameter. Image Credits: NASA/JPL-Caltech/MSSS/UofA/USGS/Calef. (For interpretation of the references to color in this figure legend, the reader is referred to the web version of this article.)

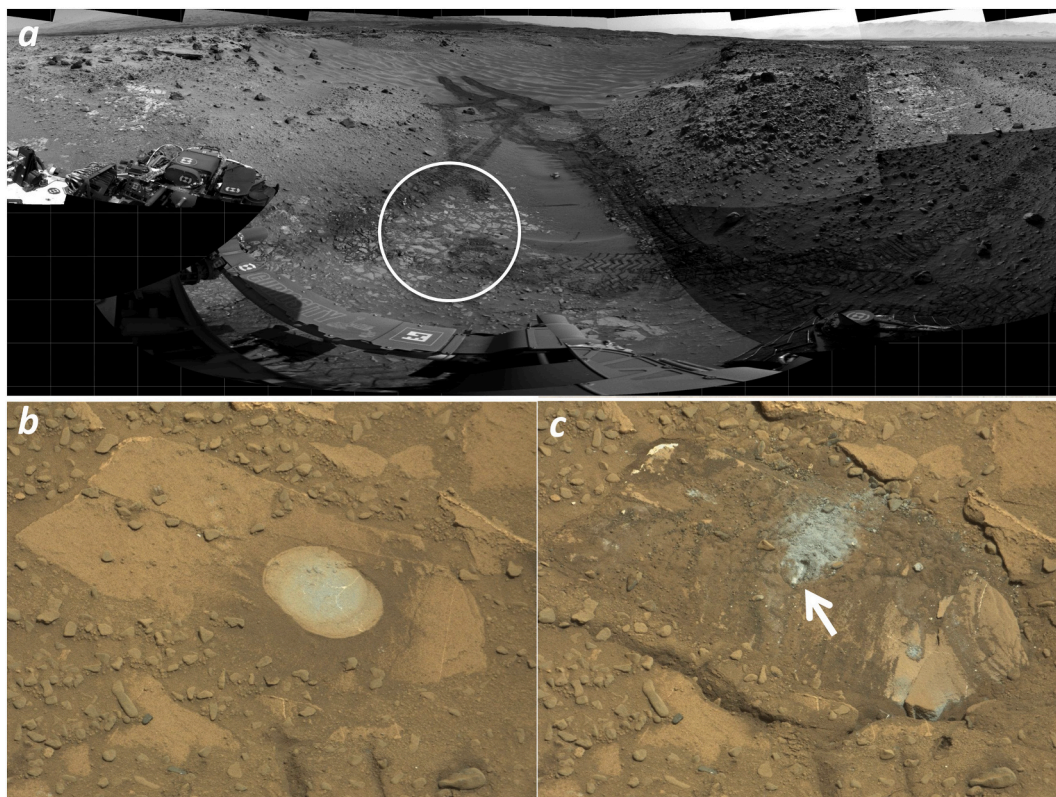


**Fig. 3.** Images from the Bonanza King drill campaign. (a) Navcam mosaic looking southwards down the northeastern ramp leading into Hidden Valley. Pale patches on ramp (white circle) include the Bonanza King mini-drill hole and full depth drill hole targets. For scale, parallel pairs of rover wheel tracks are about 2.7 m (9 ft) apart. Also of note the drill can be seen stowed on the rover arm turret in left foreground. (b) Mastcam image of Bonanza King mini-drill target acquired on Sol 722, prior to drilling attempt (0722MR0030880010402839E01). The light colored spot is where the rover's DRT removed dust from the target's surface. Spot is roughly  $4 \times 6$  cm. (c) Mastcam image of Bonanza King mini-drill target acquired on Sol 726, after drilling attempt (0726MR0031010010402920E01). Rock appears to have been pushed down and rotated along axis with the drill stabilizers, with the far side becoming depressed relative to the near side, causing a drop in preload force below the fault threshold and halting drill activity. Note the surface has also been disrupted and contaminated by sand and debris. The elongated drill hole (white arrow) is an imprint of the drill bit and does not indicate that the bit skipped or was dragged across the rock surface. Tailings generated from this aborted drill attempt were noted to have been sufficient to determine if the rock would have been safe for full depth drilling, leading to the eventual implementation of the mini-start hole as a substitute for the mini-drill hole during drill triage. *Image Credits:* NASA/JPL-Caltech/MSSS.

powder, or if there is any clumping or sticking present which could potentially clog the system. During this test, the drill stabilizers are preloaded to the surface with a force of 300 N ( $\sim 30$  kg equivalent on Earth), just as it would be for full depth drilling, testing the stability of the target. In addition, the measured parameters acquired during this test, such as rate-of-penetration (ROP), can give the engineers valuable insight as to the drillability of the target and identify rock properties including compressive strength (Peters et al., 2018). Understanding all of these parameters gives the team greater awareness of the potential risks, and provides high confidence in the safety of the hardware, before the team gives the final authorization to go forward with drilling.

During drilling, it is the SA/SPaH subsystem that is responsible for acquiring powdered sample from rock interiors and delivering these samples to SAM and CheMin (Anderson et al., 2012; Jandura, 2010). SA/SPaH is comprised of two major components, the Powder Acquisition Drill System and the sample processing unit, CHIMRA (Collection and Handling for Interior Martian Rock Analysis). The Powder Acquisition Drill System houses the Drill Bit Assembly (DBA) which cuts into rock targets using rotary percussion, a combination of hammering and rotation, which dramatically increases drilling efficiencies in semi-brittle materials, such as most rock types, and prevents excessive bit wear from rotary only drilling (Helmick et al., 2013; Okun, 2010). During drilling operations, nominal rotation is  $\sim 100$  rpm with a constant percussion frequency of about 30 Hz or 1800 blows-per-minute. It is capable of impact energies ranging from 0.05 J at Percussion Level 1 to

0.80 J at Percussion Level 6 (Table 1). A force control algorithm adjusts the position of the drill feed to maintain optimal weight-on-bit throughout drill operations. Percussion Level starts at Level 4 and is reduced if weight-on-bit cannot be maintained at the maximum feed rate. To prevent excessive bit wear, drilling operations stop altogether if the ROP ever falls below 0.025 mm/s. This strategy was designed to drill as quickly as possible at the maximum permissible Percussion Level (Level 4); sustained percussion at Levels 5 & 6 were known prior to launch to wear the percussion mechanism, and were therefore reserved for exceptional circumstances. During testing, ROP varied from the maximum of 0.25 mm/s for weak rocks composed of kaolinite and limestone to as low as  $\sim 0.02$  mm/s for strong rocks like basalt. The resultant cuttings are augured up the bit shank through a collection tube and into the sample chamber where they are held until ready for transfer into CHIMRA. The drill can acquire sample from as deep as 5 cm; however, it should be noted that, because of the DBA design, the upper  $\sim 1.5$  cm of drilled material is not collected, but instead deposited on the rock surface around the hole. Transfer of the sample from the DBA to CHIMRA is accomplished through a transfer tube using a series of turret poses in combination with percussion and vibration. Once transferred into CHIMRA, the sample is sieved and portioned into predetermined aliquots that are then transferred to the rover's analytical laboratories (Sunshine, 2010). Sample can be diverted along either the 150  $\mu$ m or the 1 mm sieve path into two separate portion chambers and subsequently delivered to SAM ( $<150$   $\mu$ m or  $<1$  mm) and/or CheMin ( $<150$   $\mu$ m only).

**Table 2**  
Target acquisition data.

Target	Sol	Start Hole		Hardness		Drilling		
		Cycles	Divot depth (mm) <sup>a</sup>	Divot depth (mm) <sup>a</sup>	Total depth (mm)	Drill-on time (s)	Avg ROP (mm/s)	
Martian year 1 <sup>b</sup>								
John Klein (mini-drill)	180	5	5.54	6.23	18.50	60	0.173	
John Klein (full drill)	182	5	5.21	5.89	63.90	400	0.144	
Cumberland (full drill)	279	4	5.08	5.97	66.25	390	0.152	
Windjana (mini-drill)	615	5	5.55	6.19	19.60	80	0.136	
Windjana (full drill)	621	5	5.10	5.72	65.08	560	0.105	
Martian year 2								
Confidence Hills (mini-drill)	756	4	5.62	6.50	19.88	50	0.239	
Confidence Hills (full drill)	759	5	5.72	6.58	65.82	320	0.184	
Mojave (mini-drill)	867	4	6.08	6.97	19.69	40	0.236	
Mojave 2 (mini-drill)	881	4	4.96	5.67	19.88	50	0.238	
Mojave 2 (full drill) <sup>c</sup>	882	6	4.88	NA	65.04	590	0.099	
Telegraph Peak (full drill)	908	6	5.50	NA	65.86	662	0.090	
Buckskin (mini-start)	1059	3	3.20	4.10	–	–	–	
Buckskin (full drill)	1060	7	6.43	NA	64.50	680	0.082	
Big Sky (mini-start)	1116	4	4.38	4.72	–	–	–	
Big Sky (full drill)	1119	7	5.22	NA	64.40	724	0.080	
Pilgrim (mini-start)	1134	4	4.49	5.13	–	–	–	
Greenhorn (full drill)	1137	7	4.77	NA	65.32	710	0.084	
Lubango (full drill)	1320	7	5.22	NA	65.27	770	0.076	
Okoruso (full drill)	1332	7	4.95	NA	65.11	700	0.085	
Martian year 3								
Oudam (full drill)	1361	7	5.34	NA	65.29	750	0.078	
Marimba (full drill)	1422	7	4.88	NA	65.15	820	0.072	
Quela (full drill)	1464	5	5.35	NA	63.94	610	0.094	
Sebina (full drill)	1495	7	5.10	5.41	65.38	680	0.087	

<sup>a</sup> Total Drill Hole Depth after Start Hole procedure and Hardness Test, respectively (NA indicates Hardness Test was not performed).

<sup>b</sup> Drilling data for Curiosity's first Martian year are described in more detail in [Abbey et al. \(2019\)](#).

<sup>c</sup> From this point forward, all full depth drill holes were made using the reduced percussion protocol.

Nominal drilling protocol dictates that each drill hole, both mini and full depth, be preceded by the creation of a Start Hole and a Rock Hardness Test ([Helmick et al., 2013](#); [Okun, 2010](#)). The Start Hole procedure creates a shallow hole to guide the drill bit during the start of drilling operations, keeping the bit on-axis and ensuring it does not encounter excessive side loading, which can result in drill failure as the bit goes deeper and side loads increase. This procedure begins by contacting the rock surface with the bit and percussing for a short period at Percussion Level 3, before retracting, rotating a small increment (22.5°), contacting the surface again, percussing, and so on until an 'asterisk pattern' is chiseled into the surface. It then enters a clear-out phase in which the bit is rotated while lightly percussing. This process slowly chips away surface topography, continuing until the entire surface area of the hole has been removed. The next step is to rotate the bit, while lightly percussing, to clear away any cuttings that have accumulated. In this way, a smooth-bottomed hole is created which aids drilling. This entire cycle is repeated until the start hole reaches a depth of at least 4.5 mm below the highest surface contact point. This typically takes 4 to 6 cycles. Following Start Hole creation, but prior to actual drilling, a Hardness Test is commonly performed to assess the hardness of the drill target. It consists of several techniques used in succession to create an indentation at the bottom of the Start Hole. First, the drill bit is pressed into the rock using 130 N (~13 kg equivalent on Earth) of force. Second, a tap test is performed with a single percussive burst. Finally, a series of percussive bursts are applied at each Percussion Level from 1 to 6. While an absolute hardness is difficult to determine with this technique, the depth of the resultant divot can be evaluated and qualitatively compared with rocks previously examined. In the testbed, final indentation depths ranged from ~0.8 mm for soft rocks composed of kaolinite and limestone to ~0.4 mm for hard rocks like basalt.

### 3. Bonanza king and the revised drilling protocol

Curiosity's first unsuccessful drill attempt was made early in the

second Martian year on a rock dubbed 'Bonanza King' (Sol 724) in the mouth of Hidden Valley ([Figs. 2 & 3](#)). It cropped out as a low-lying patch of exposed rock that was lighter toned, less resistant, and finer-grained than the sandstones the rover had previously been driving over during much of the first Martian year (e.g. Windjana) and the team felt it was important to document this transition. Furthermore, Bonanza King occurred at a similar elevation to the rocks at Pahrump Hills at the base of Mt. Sharp, suggesting a possible stratigraphic correlation ([Grotzinger et al., 2015](#)). Determining the composition of this sample could potentially provide a better understanding of the types of rocks the team would find at the base of Mt. Sharp. In addition, new algorithms had been developed to shorten drill time and a team wide exercise was planned to refine drilling protocols so a sample could be acquired with higher efficiency and lower impact to both strategic goals and the normal operational timeline. This condensed drilling exercise was to be tested for the first time at Bonanza King.

One point of concern at this site was that similar nearby patches of rock became fractured when the rover drove over them. This raised the possibility that the proposed drill target might not consist of exposed bedrock, but rather thin layers of rock that may easily fracture upon drilling. If the targeted rock fractured and the drill's collection tube failed to make a good seal with the edges of the drill hole, little or no sample would be acquired. While additional preload tests were performed to alleviate some of these concerns, it was realized that the risk of failure was high at this site. But the target was deemed to be of high scientific value by the science team and it was determined there was little risk to the SA/SPaH hardware, so it was decided to go forward with testing. On Sol 724 a mini-drill hole was created approximately 15 cm away from the proposed Bonanza King full depth drill target on a neighboring flagstone ([Fig. 3b](#)). However, the Start Hole process terminated after completing 3 of the expected 5–6 cycles, penetrating <3.5 mm. Drilling was halted automatically by the system's fault protection protocol after the preload force on the drill stabilizers dipped below the drill's 150 N fault threshold. Arm force sensors recorded that

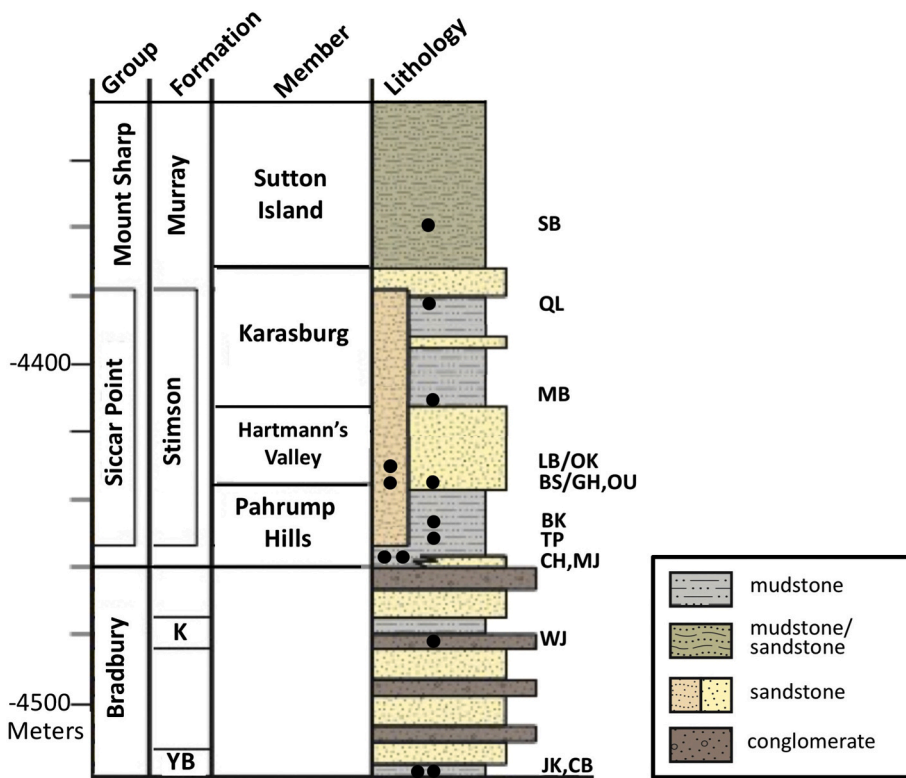


Fig. 4. Stratigraphic column for the sedimentary rocks encountered at Gale crater through the end of the third Martian year, modified after Fedo et al. (2018) & Grotzinger et al. (2015). Full depth drill holes are indicated by solid black circles: JK, John Klein; CL, Cumberland; WJ, Windjana; CH, Confidence Hills; MJ, Mojave 2; TP, Telegraph Peak; BK, Buckskin; BS/GH, Big Sky/Greenhorn; LB/OK, Lubango/Okoruso; OU, Oudam; MB, Marimba; QL, Quela; SB, Sebina. K is Kimberley and YB is Yellowknife Bay. Elevations are referenced to the zero-elevation datum on Mars as defined by Smith et al. (2001).

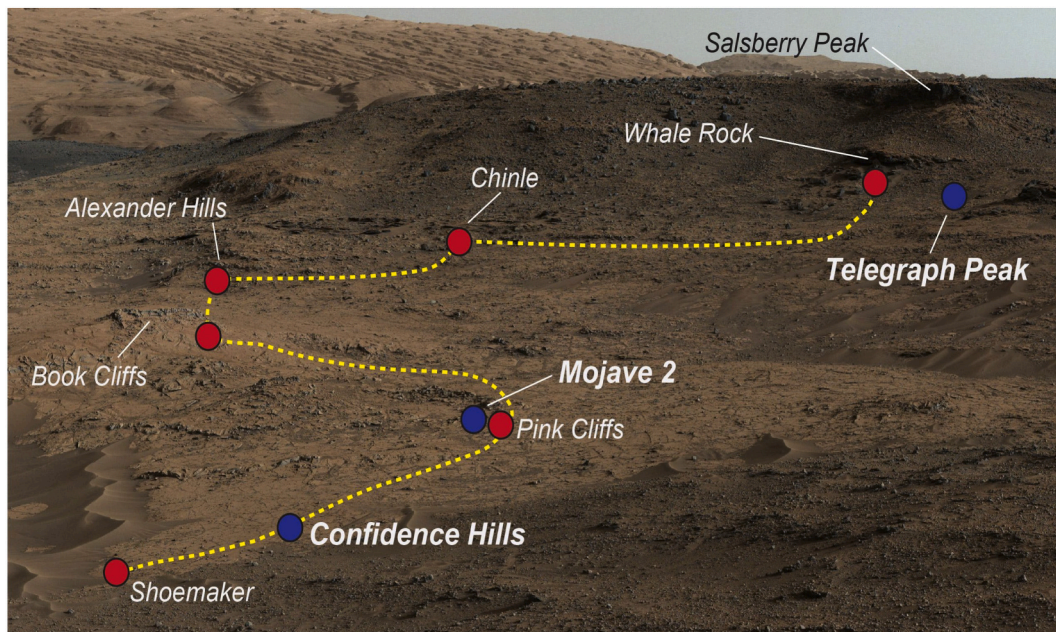
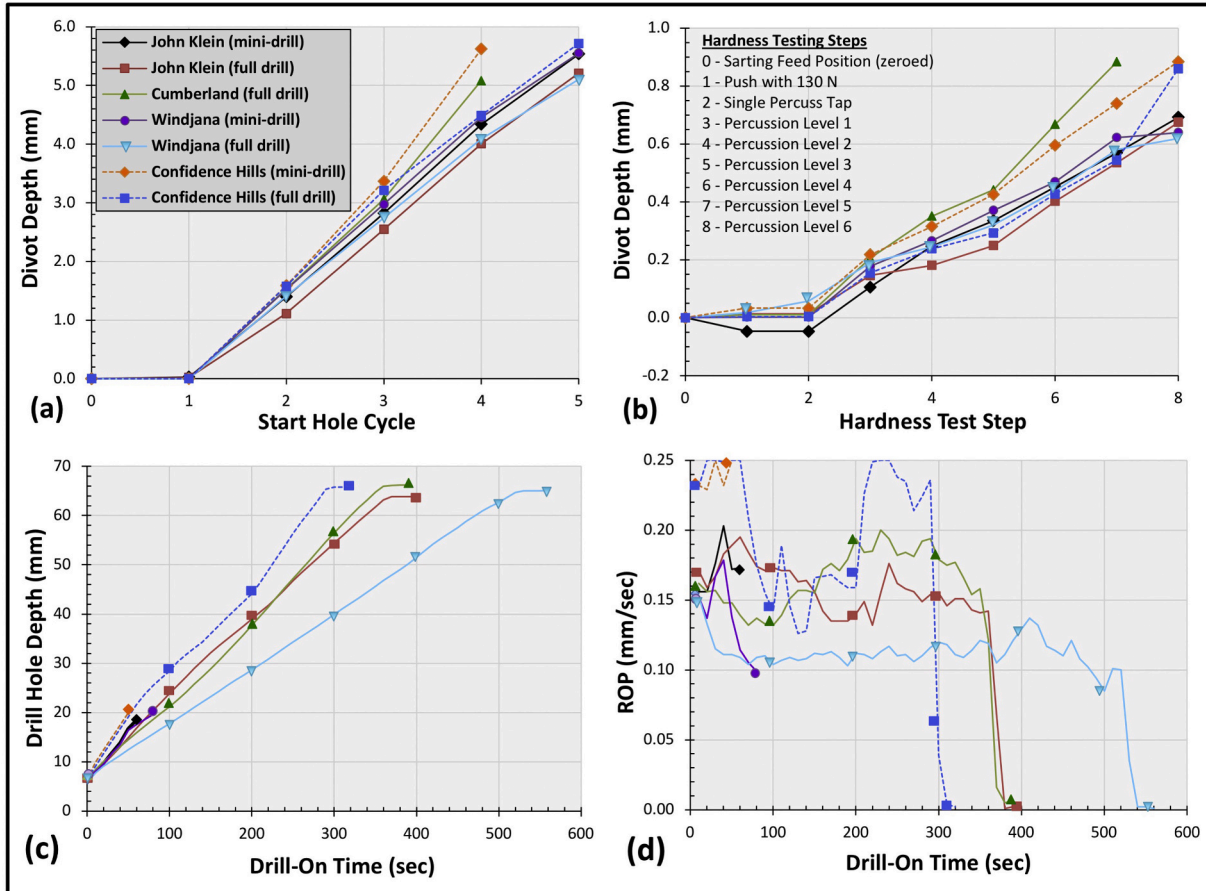
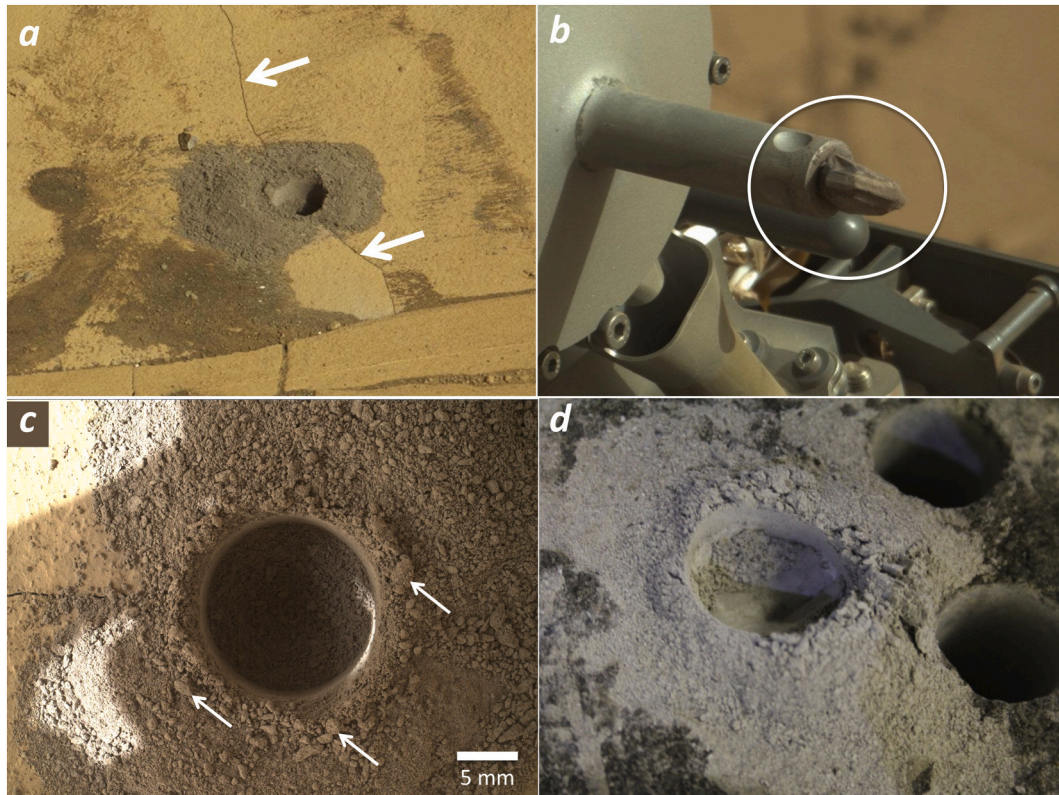


Fig. 5. Mastcam mosaic showing the Pahrump Hills section of the Murray formation, where approximately 18 m of mudstone layers are exposed. The dotted yellow line shows the route of the chemostratigraphic survey (i.e. 'walkabout') that was conducted after drilling an initial full depth drill hole at Confidence Hills. Observations made during this walkabout informed the selection of the final two full depth drill targets at Mojave 2 and Telegraph Peak. Red circles indicate other targets of interest closely inspected during the walkabout and blue circles indicate the drill sites. The camera is approximately 20 m northwest of the outcrop, looking southeast. This scene is a portion of the Mastcam mosaic acquired on Sol 751 (PIA18608). Image Credit: NASA/JPL-Caltech/MSSS. (For interpretation of the references to color in this figure legend, the reader is referred to the web version of this article.)



**Fig. 6.** Graphs showing target acquisition data for standard percussion targets. Targets from MSL’s first Martian year (Abbey et al., 2019) are also included here for comparison and completeness. (a) Start Hole Cycle vs Cumulative Divot Depth. (b) Hardness Test Step vs Cumulative Divot Depth. Note Mojave mini-drill hole terminated the Hardness Test before completing Step 8 due to reaching a maximum Divot Depth of 0.9 mm. (c) Drill-On Time vs Drill Hole Depth. (d) Drill-On Time vs Rate of Penetration (ROP). Initial Drill Hole Depth is the total combined Divot Depth created by the Start Hole process and Hardness Test (see Table 2). Note the sudden drop in Rate of Penetration at the bottom of the full depth drill holes signifying that maximum depth was achieved. Also note that Confidence Hills (mini-drill) and Mojave 2 (mini-drill) have almost identical ROP profiles, so cannot be resolved in this graph.



**Fig. 7.** Images from the Confidence Hills mini-drill hole test acquired on Sol 756 demonstrating that behavior of the mini-drill tailings is consistent with that of fine dry particulate material. (a) Mastcam image shows ‘classic’ tailings pile similar to those formed under dry conditions (0756MR0032500010403769E01). The fracture (white arrows) formed during mini-drill percussion and suggests this target may be a thin plate or flagstone rather than solid bedrock. Also note the darker toned fine dust emanating from the contact between the plates, likely mobilized by mini-drill percussion. (b) Mastcam image of drill bit after drilling (white circle) shows minimum amount of powder sticking to hardware (0756MR0032520000403767E01). (c) MAHLI image, taken from a standoff distance of 5 cm, shows clumps formed in tailings during drilling (white arrows) (0756MH0004220000204604R00). They appear to disaggregate further away from the drill hole. Similar behavior, probably due to electrostatics, has been observed in the testbed under Mars ambient conditions during drilling and processing of both sedimentary and igneous rocks. (d) Weathered basalt mini-drilled in testbed under low humidity ( $-70^{\circ}\text{C}$ ) conditions showing similar clumps, as well as ‘classic’ tailings pile formation. Clumps readily disaggregate with movement and/or vibration. Note in all images drill bit and drill holes are 1.6 cm in diameter. *Image Credits:* NASA/JPL-Caltech/MSSS.

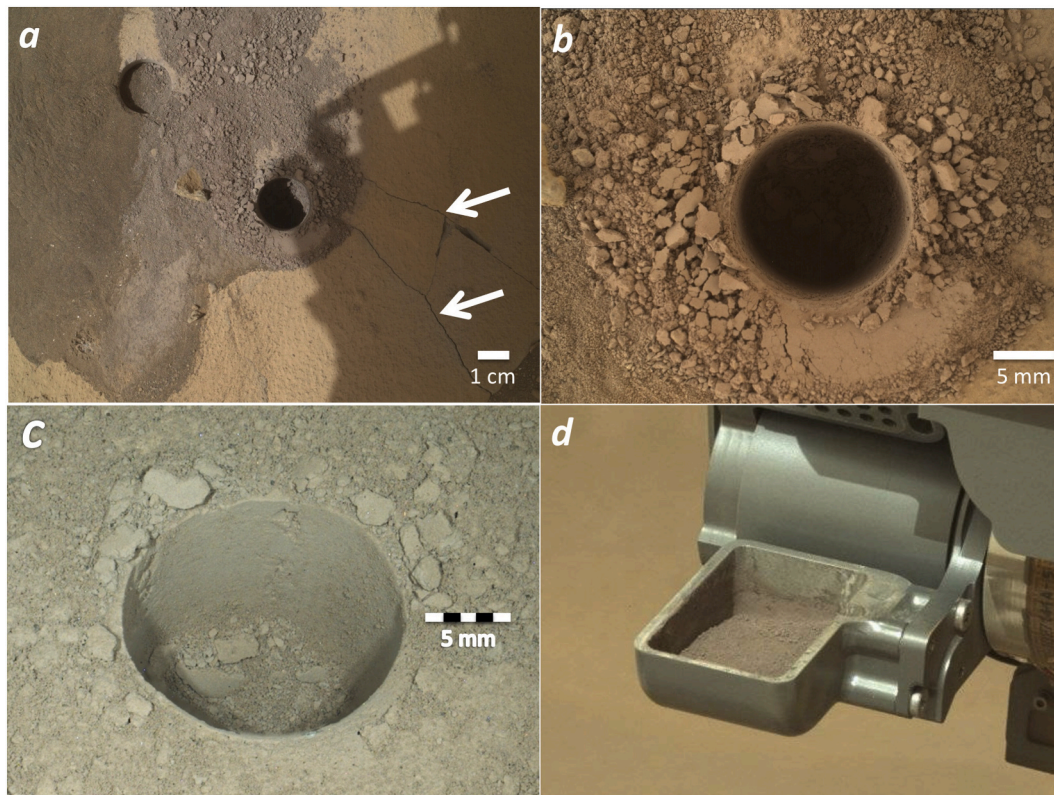


**Fig. 8.** Images from the Confidence Hills full depth drill campaign. (a) MAHLI image of both full depth drill hole (center) and mini-drill test hole (upper left) taken at a standoff distance of 25 cm on Sol 759 (0759MH0003970010300030C00). New fractures (white arrows) formed during percussion, but did not compromise the integrity of the drill hole. (b) MAHLI image of full depth drill hole taken at a standoff distance of 5 cm on Sol 759 (0759MH0004290000300074R00). Note the partial flattening of the tailings pile immediately surrounding the drill hole. This is due to the DBA making contact with the tailings pile when the drill reaches full depth. (c) MAHLI image of full depth drill hole taken from oblique angle on Sol 768 (0771MH0004350000300252R00). Apparent color difference of tailings is due to this image being acquired at night under white light LED illumination. (d) Mastcam image of processed sample in scoop acquired on Sol 762 (0762ML0032750000400106E01). Note in all images drill hole is 1.6 cm in diameter. Scoop is 4.5 cm wide. *Image Credits:* NASA/JPL-Caltech/MSSS.

weight-on-bit gradually declined from 240 N to 150 N during drill motion, most likely due to the rock being pushed down into the underlying sediment and rotating slightly during start hole percussion (Fig. 3c). This was deemed a ‘successful failure’ as the rover fault protections performed as expected and the drill triage protocol provided the team with valuable insight into whether or not full depth drilling should be attempted at this location. After careful deliberation, the team concluded that, based on these results, the Bonanza King target was an unacceptable candidate for drilling and no further attempts were made to drill the rock. However, while ultimately not collecting nor providing any sample to the instruments for analysis, the condensed drilling exercise was considered a success and the team gained new experience and ideas on how to improve the pace of drilling in the future. Additionally, this was the first successful implementation of fault protections during drilling on Mars. Confidence was gained in the hardware and in picking drill targets of high scientific relevance that could potentially slip or crack during the drilling process without damaging the hardware.

### 3.1. Reduced percussion protocol & mini-start hole procedure

In response to the Bonanza King incident, and in anticipation of encountering less resistant, more weakly consolidated rocks during the climb up Mt. Sharp, such as those drilled early in the mission at Yellowknife Bay, the engineering team quickly developed a more adaptive drilling algorithm that would impart less percussive force on future drill targets, particularly at the start of drilling, hopefully reducing any chance of fracturing the rock at these locations. This new reduced

percussion algorithm would begin both the Start Hole procedure and full depth drilling at Percussion Level 1 and step up percussion only when the ROP falls below 0.05 mm/s and step down when the ROP rises above 0.13 mm/s. To prevent excessive bit wear, as with the original algorithm, drilling operations stop altogether if the ROP ever falls below 0.025 mm/s. In addition, the reduced percussion algorithm forgoes the Hardness Test to further minimize the total percussive force applied to the target (although it would be added back on Sol 1495 for the Sebina target). The new reduced percussion protocol was first deployed during the Pahrump Hills campaign when it was successfully used to drill a full depth drill hole into the Mojave 2 target on Sol 882 (see below). It should be noted that an added benefit of using the reduced percussion protocol is that its step-wise increase in Percussion Level enables estimation of the uniaxial compressive strength of any rocks drilled to full depth using this technique (Peters et al., 2018).

In addition to the reduced percussion protocol, other refinements were made as a result of the Bonanza King drill attempt. Significantly, it was observed by the team that the tailings created by the aborted Start Hole would have been sufficient to determine if their behavior was consistent with that of a dry granular powder and therefore safe for ingestion by the SA/SPaH hardware. This was despite the fact that the Start Hole penetrated <3.5 mm into the target, whereas the mini-drill hole normally used to make this determination typically creates a hole almost 2 cm deep into the target. This observation eventually led to the adoption of the new mini-start hole procedure as a replacement for the original mini-drill hole procedure starting with the Buckskin target on Sol 1059. It should be noted that the mini-start hole described here is

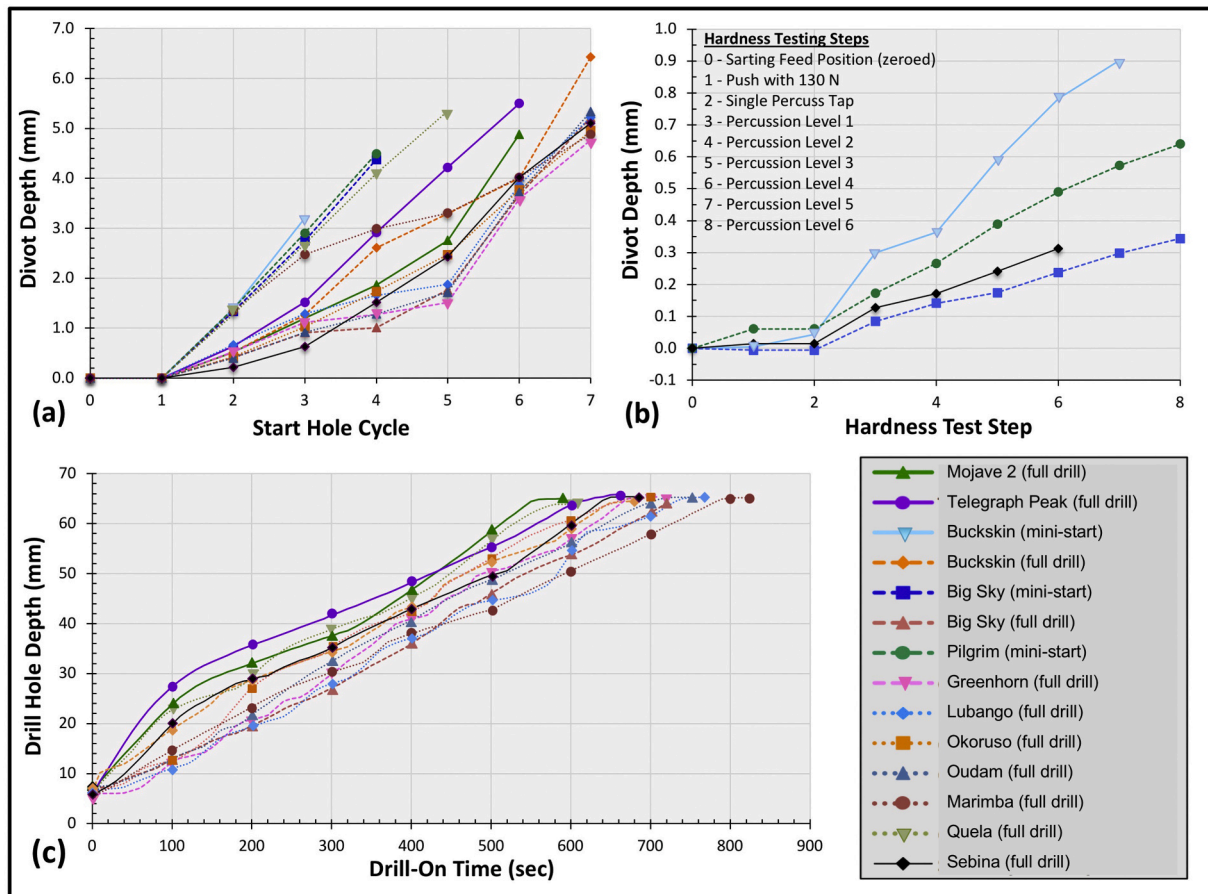


Fig. 9. Graphs showing target acquisition data for reduced percussion targets. (a) Start Hole Cycle vs Cumulative Divot Depth. Note mini-start hole targets, as well as Marimba and Quela full depth drill holes, began their Start Hole procedure at Percussion Level 3, whereas all others began at Level 1. (b) Hardness Test Step vs Cumulative Divot Depth. Note Buckskin mini-start hole terminated the Hardness Test before completing Step 8 due to reaching a maximum Divot Depth of 0.9 mm. Also, the Sebina full depth drill hole Hardness Test was terminated at Percussion Level 4 (Step 6) to mitigate degradation of drill system hardware. (c) Drill-On Time vs Drill Hole Depth. Initial Drill Hole Depth is the total combined Divot Depth created by the Start Hole process and Hardness Test (see Table 2). Note Drill-On Time vs Rate of Penetration (ROP) for reduced percussion targets is presented in Fig. 12.

separate and distinct from the full Start Hole used as a precursor to mini and full depth drilling. To compare, the full Start Hole creates a divot of at least 4.5 mm depth, frequently reaching >5 mm below the highest surface contact point, while the mini-start hole creates a much shallower divot, only reaching a depth of about 3 mm. The mini-start hole test was originally developed during testbed experiments on Earth but, up to this point, had not been deployed during actual drill operations on Mars. It is worth noting that, unlike the reduced percussion protocol, the mini-start hole consistently operates at Percussion Level 3 and utilizes the Hardness Test.

4. Results from drilling

The second Martian year began with the Curiosity rover transitioning from the sandstone-dominated rocks of Bradbury Rise, on the plains of Aeolis Palus, to the foothills and rocks of Mt. Sharp (i.e., Aeolis Mons), where the team got its first look at the fine-grained, laminated mudstones of the Murray formation and the coarser-grained sandstones of the Stimson formation (Fig. 2). During the course of the second Martian year, eight full depth drill holes were successfully made in these foothills. The first four, dubbed ‘Confidence Hills’ (Sol 759), ‘Mojave 2’ (Sol 882), ‘Telegraph Peak’ (908) and ‘Buckskin’ (Sol 1060), were made in the Murray formation in the Pahrump Hills and Marias Pass regions of the crater. The second four, dubbed ‘Big Sky’ (Sol 1119), ‘Greenhorn’ (Sol 1137), ‘Lubango’ (Sol 1320) and ‘Okoruso’ (Sol 1332) were made in

the Stimson formation in the Bridger Basin and Naukluft Plateau regions. During the course of the third Martian year, four additional full depth drill holes, dubbed ‘Oudam’ (Sol 1361), ‘Marimba’ (Sol 1422), ‘Quela’ (Sol 1464) and ‘Sebina’ (Sol 1495), were successfully made in the Murray formation west of the Naukluft Plateau and in the Murray Buttes region. Drill data acquired for each target is summarized in Table 2 and discussed in detail below.

The second Martian year, as noted above, marked the development and execution of the reduced percussion algorithm and the adoption of the mini-start hole as an ersatz proxy for the mini-drill test. It’s worth mentioning that these and other refinements helped contribute to a much faster turnaround time between given drill campaigns, with only 12 sols separating the acquisition of the Lubango and Okoruso full depth drill samples. However, despite these improvements, the second Martian year was not trouble free. The most notable setback came on Sol 911 when an electrical short in the percussion mechanism occurred during sample transfer. The Engineering Team had to implement significant mitigations to the now-standard Reduced Percussion Protocol: 1) battle short current fault limits were set to be tolerant of shorting events; 2) motor controller flight software was patched to a) improve the speed of the fault response, and b) maintain visibility of shorting events below the fault threshold; 3) high-speed recording of percussion and battle shorts was enabled around percussion uses; and 4) the sequence and operations process was modified to permit, should a shorting event fault the drill, restarting the drill attempt in the same hole on a subsequent

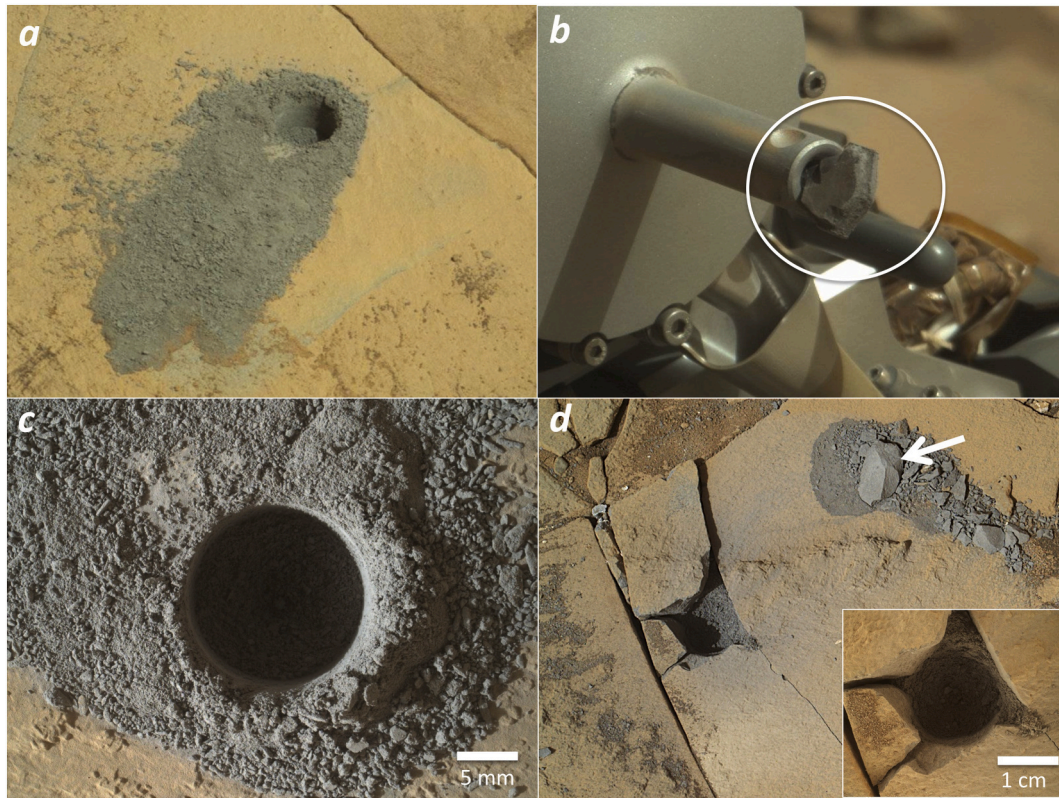


**Fig. 10.** Images from the Mojave & Mojave 2 mini-drill hole tests demonstrating that behavior of the mini-drill tailings is consistent with that of fine dry particulate material. (a) Mastcam image of Mojave 2 mini-drill tailings pile acquired on Sol 881 shows tailings flowing over pre-existing topography (0881MR0038450010501178E01). (b) Mastcam image of drill bit after Mojave 2 mini-drill testing (white circle) acquired on Sol 881 shows only minor amounts of material cohered to the bit tip (0881MR0038470000501176E01). This is consistent with testbed results and experience has demonstrated that this material would likely be removed during vibration when sample is transferred to CHIMRA. (c) MAHLI image of Mojave 2 mini-drill tailings pile, taken from a standoff distance of 5 cm on Sol 881, shows ‘classic’ tailings pile and clumping, most likely due to electrostatics, similar to that seen at Confidence Hills and in the testbed (0881MH0004220000302452R00). (d) MAHLI image of Mojave mini-drill test, taken from a standoff distance of 35 cm on Sol 867, showing fracture of mini-drill target and debris (white arrow) ejected from hole (0867MH0004240010302170C00). This result leads to a second mini-drill test being conducted at Mojave 2. Inset: MAHLI image of same taken from a standoff distance of 5 cm (0867MH0004220000302173R00). Note in all images drill bit and drill holes are 1.6 cm in diameter. *Image Credits:* NASA/JPL-Caltech/MSSS.

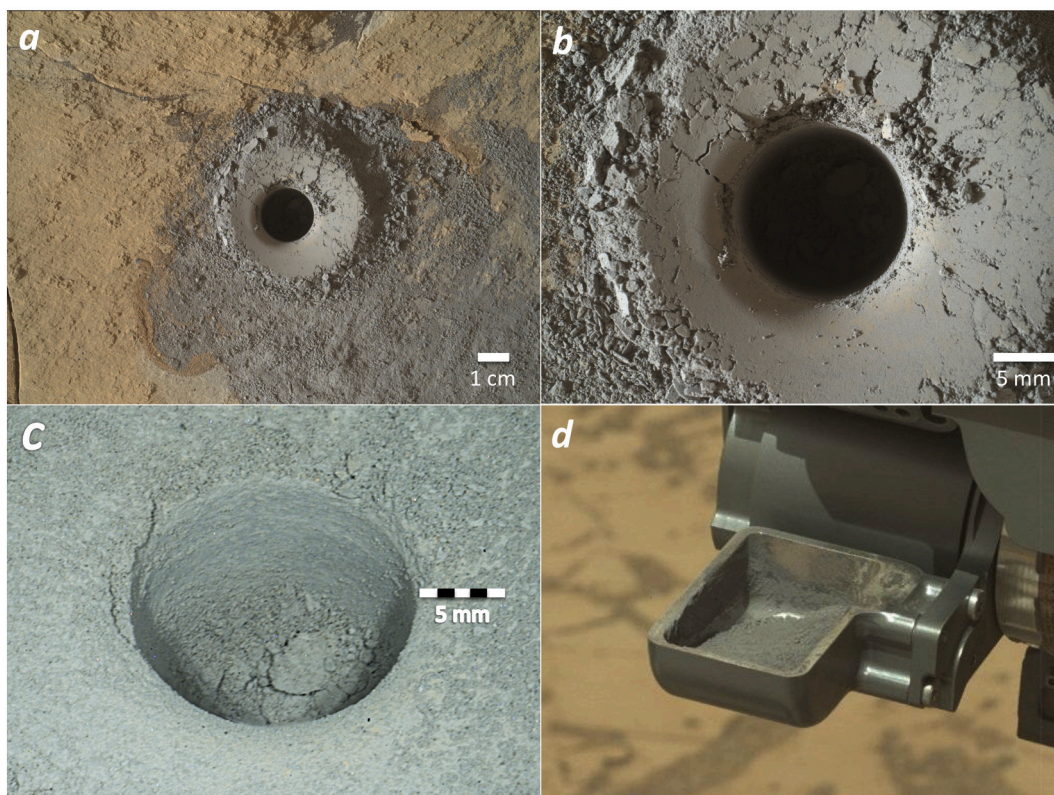


**Fig. 11.** Images from the Mojave 2 full depth drill campaign. (a) MAHLI image of full depth drill hole taken at a standoff distance of 25 cm on Sol 882 (0882MH0003970010302481C00). (b) MAHLI image of full depth drill hole taken at a standoff distance of 5 cm on Sol 882 (0882MH0004230000302526R00). Note that clumps, like those seen in the mini-drill test, are readily flattened and disaggregated upon contact with the DBA, confirming their electrostatic nature. (c) MAHLI image of full depth drill hole taken from an oblique angle on Sol 883 (0884MH0004660000302639R00). Image acquired at night under white light LED illumination. (d) Mastcam image of processed sample in scoop acquired on Sol 884 (0884ML0038540000401817E01). Note in all images drill hole is 1.6 cm in diameter. Scoop is 4.5 cm wide. *Image Credits:* NASA/JPL-Caltech/MSSS.

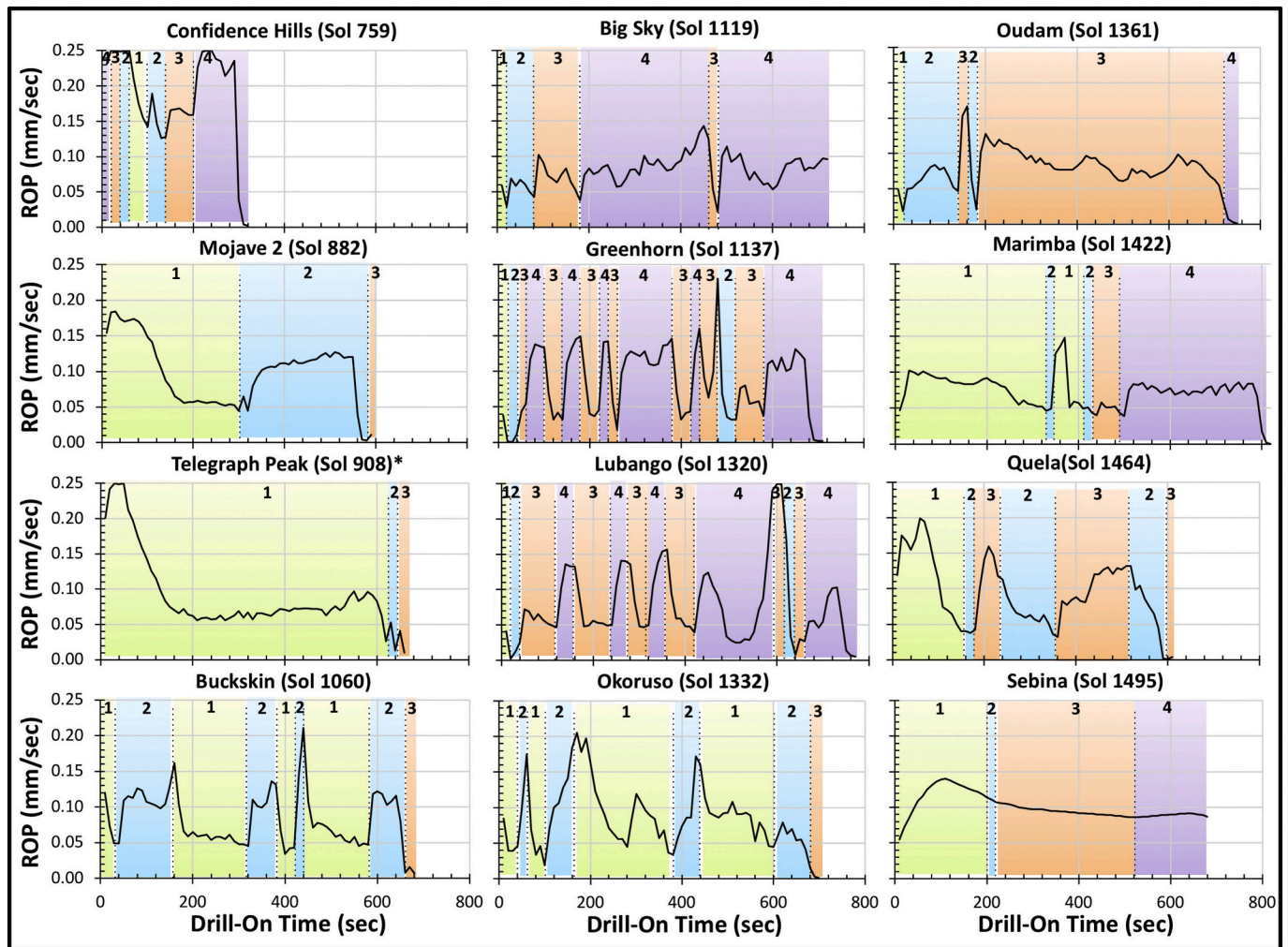
day (however, we never needed to employ this option during operations). Afterwards, periodic shorting events while percussing plagued the second and third year drilling campaigns. Realizing that the ability to percuss during drilling and sample transfer may one day be unavailable, an effort was begun to develop a full depth drilling method that did not require percussion. As noted previously, the engineering team was also aware that higher Percussion Levels (5 & 6), and their higher energy outputs, may prematurely degrade the capability of the drill system. As a way to mitigate (or at least delay) further degradation of the drill hardware, it was decided that future operations would have their Percussion Levels capped at Level 4, with the exception of the brief Hardness Test performed during the mini-start hole procedure. However, despite these precautions, intermittent shorts continued to occur (Sols 1121, 1323, 1362, 1423 & 1461). Most notably, on Sol 1423 (Marimba) transfer of sample was delayed due to multiple (16 total) percussion-related shorts. In response to the observed increase and severity of these shorts, and the fact that up to this point they had only occurred during sample transfer, it was decided that future sample transfers would be performed using vibration only without the use of percussion. However, at the very next drill target, on Sol 1461 (Quela), drilling was aborted when another percussion-related short was detected. This time it occurred during initiation of the Start Hole procedure, totally unrelated to sample transfer. Thus, on Sol 1536, the engineering team decided that it was time to test the new non-percussive full depth drilling algorithm. The results of this unsuccessful attempt are described in Section 5.

In the third Martian year, sampling was limited to four additional full depth drill holes. This was primarily due to a fault in the drill feed

mechanism that presses the drill into a rock after the stabilizers are preloaded. Ironically, this drill feed fault was not directly associated with the shorting events described above. However, the drill feed mechanism's first failure did occur during testing of the new non-percussive full depth drilling algorithm.

#### 4.1. Pahrump Hills (Martian year 2)

Confidence Hills, Mojave 2 and Telegraph Peak were the fourth, fifth and sixth rocks successfully drilled on Mars. These rocks are part of the Murray formation in the Pahrump Hills region of Gale crater and lie at a higher elevation than the rocks previously drilled in the Yellowknife Bay and Kimberley formations (Fig. 4). They consist primarily of fine-grained, laminated mudstones and represented our first chance to directly sample rocks from the base of Mt. Sharp. The science team was interested in learning about the Murray formation's depositional environment, its history of water-rock interactions, potential to preserve organics, and the nature of its stratigraphic relationship with the underlying sandstones of Bradbury Rise. The location chosen for this campaign consists of over 10 m of well exposed stratigraphy representing some of the lowest elevation exposures of Mt. Sharp deposits (Fig. 5). The plan was to collect the first sample upon arrival from the lowest part of the section and then perform a chemo-stratigraphic survey, or 'walkabout', of the rest of the section using context imaging and ChemCam. The information gathered from this reconnaissance would aid the team in choosing context science targets for analysis by MAHLI and APXS during a second pass over the section. The collective data would then be used to select drill targets, akin to the way a field



\*note the last 2 sec of Telegraph Peak utilized Percussion Level 4 (not pictured)

**Fig. 12.** Drill-On Time vs Rate-of-Penetration (ROP) for full depth drill holes created during second and third Martian year. All drill holes were created using reduced percussion protocols with the exception of Confidence Hills, which used standard percussion and is included here for the sake of comparison. Colors correspond to Percussion Level utilized for the indicated time period: green = Level 1, blue = Level 2, orange = Level 3, purple = Level 4. Note that most targets show a sudden drop in ROP at the bottom of the drill holes signifying maximum depth was achieved. (For interpretation of the references to color in this figure legend, the reader is referred to the web version of this article.)

geologist walks an outcrop before collecting samples. The bulk chemical composition of these rocks suggested they are composed of a mixture of mafic phases consistent with basaltic-derived sediments (Thompson et al., 2016; Wiens et al., 2016). Vein material is generally enriched in S and Ca compared to other targets, suggesting they are dominated by relatively pure Ca-sulfate (i.e., gypsum, bassanite, anhydrite) (L'Haridon et al., 2018; Nachon et al., 2017). Extensive testbed experience drilling into weathered basaltic materials, as well as Ca-sulfate samples, suggested to the team that there was little danger to the SA/SPaH system if drilling was attempted at this location. Our drilling experience during the first Martian year into similar rocks at Yellowknife Bay gave us additional confidence in this assessment (Abbey et al., 2019).

#### 4.1.1. Confidence Hills

The first full depth drill site chosen for the Pahrump Hills campaign was in the lowest part of the exposed Murray formation (Fig. 4). On Sol 756 a mini-drill hole was created approximately 5–6 cm away from the proposed Confidence Hills full depth drill target. The Start Hole process took 4 cycles to penetrate >4.5 mm (which is typical based on previous drill holes), reaching a depth of 5.62 mm, at Percussion Level 3 (Fig. 6a). The Hardness Test increased the divot depth by 0.88 mm to a total of

6.50 mm (Fig. 6b). The mini-drill penetrated the surface to a total depth of 19.88 mm in 50 s total drill-on time with a cumulative average rate of penetration of 0.239 mm/s at Percussion Levels 4 (0–10 & 30–50 s) and 5 (10–30 s) (Fig. 6c & d). This is very close to the top drilling speed of 15 mm/min (0.25 mm/s), suggesting that the Confidence Hills target was relatively soft and would be easy to penetrate (Peters et al., 2018). Furthermore, the behavior of the mini-drill tailings was entirely consistent with that of a dry granular powder (Fig. 7), giving the team confidence that this material would pose little risk to flight hardware. One point of concern was a fracture that formed during mini-drill percussion, suggesting that this target may be a thin plate or flagstone rather than solid bedrock, posing the question as to whether the drill had ‘punched through’ the rock into underlying loose sediment. However, like at Bonanza King, it was determined that this posed little risk to the drill itself, and would only compromise our ability to collect sample, so the science team decided to go forward with full depth drilling. It is worth noting that this constituted the last use of the original drilling protocol before the team switched to the new reduced percussion algorithm.

On Sol 759 the team commenced with full depth drilling and caching of the Confidence Hills sample (Fig. 8). The Start Hole process took

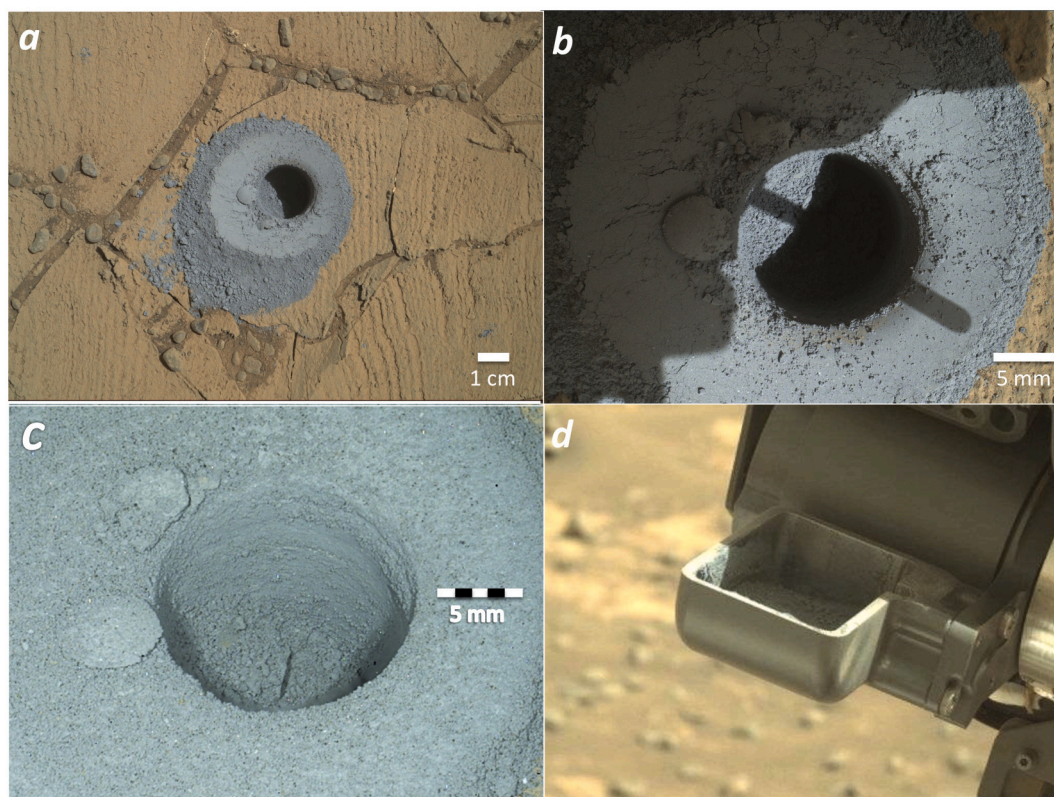


**Fig. 13.** Images from the Telegraph Peak full depth drill campaign. (a) MAHLI image of full depth drill hole taken at a standoff distance of 25 cm on Sol 908 (0908MH0003970010302871C00). (b) MAHLI image of full depth drill hole taken at a standoff distance of 5 cm on Sol 908 (0908MH0004230000302918R00). A shadow from the MAHLI poker can be seen prominently dissecting the drill hole. (c) MAHLI image of full depth drill hole taken from an oblique angle on Sol 910 (0911MH0004750000303059R00). Image acquired at night under white light LED illumination. (d) Mastcam image of processed sample in scoop acquired on Sol 922 (0922ML0040440000402709E01). Note in all images drill hole is 1.6 cm in diameter. Scoop is 4.5 cm wide. *Image Credits:* NASA/JPL-Caltech/MSSS.

5 cycles to reach a depth of 5.72 mm at Percussion Level 3 (Fig. 6a). The Hardness Test results were comparable to those of the mini-drill hole, increasing the divot depth by 0.86 mm to a total depth of 6.58 mm (Fig. 6b). The full drill penetrated the surface to a maximum total depth of 65.82 mm in 320 s total drill-on time with a cumulative average rate of penetration of 0.184 mm/s and a maximum Percussion Level of 4 (Fig. 6c & d) and it is interesting to note that the ROP became so fast that the feed could not keep up, so the algorithm had to reduce the Percussion Level (Figs. 6d & 12). On Sol 762 the sample was transferred from the DBA to CHIMRA and into the scoop where it was estimated that  $15.7 \pm 1.3 / -0.3 \text{ cm}^3$  of material had been collected based on CAD models (Fig. 8d). This was as expected for a full depth drill hole. The sample was then processed through the  $150 \mu\text{m}$  sieve path and a portion was delivered to CheMin on the same sol. Subsequently, portions were delivered to SAM on Sols 765 and 773. CheMin results showed that Confidence Hills is rich in pyroxene, phyllosilicates and hematite, with minor amounts of magnetite, apatite and jarosite (Rampe et al., 2017a). The presence of jarosite, a mineral that forms under acidic environments ( $\text{pH} < 4$ ) (e.g., Driscoll and Leinz, 2005), and abundant hematite suggests that the Murray mudstones in the Pahrump Hills area may have been exposed to acidic/oxidizing conditions after deposition. However, the presence of apatite, which is not stable under acidic conditions (e.g., Chairat et al., 2007), is difficult to reconcile and suggests that the sediments of the Murray formation in this region have a complex geochemical history. In addition, SAM analyses also detected the presence of thiophenic, aromatic, and aliphatic compounds in both this sample and the Mojave 2 sample described below (Eigenbrode et al., 2018). The preservation of these organic compounds was likely aided by vulcanization, a process by which sulfur structurally links the organic material into a macro-molecule that is more resistant to oxidation than

the organics by themselves. Detection of these compounds close to the Martian surface, where ionizing and oxidizing conditions are at their harshest, indicates that organic material can be preserved just below the surface.

#### 4.1.2. Mojave & Mojave 2

Mojave was chosen as the second full depth drill target at Pahrump Hills due to the presence of fine lenticular features, tentatively interpreted as diagenetic crystals (possibly pseudomorphs) (Kah et al., 2018). It was located less than a meter up section from Confidence Hills (Fig. 4). On Sol 867 a mini-drill hole was created approximately 5 cm away from the proposed Mojave full depth drill target. The Start Hole process took 4 cycles to reach a depth of 6.08 mm at Percussion Level 3 (Fig. 9a). The Hardness Test increased the divot depth by 0.89 mm to a total of 6.97 mm (Fig. 9b). The mini-drill penetrated the surface to a total depth of 19.69 mm in 40 s total drill-on time with a cumulative average rate of penetration of 0.236 mm/s at Percussion Levels 5 (0–20 s) and 4 (20–40 s) (Fig. 9c). While these results were comparable to those of the Confidence Hills target, the Mojave slab fractured during testing, most likely due to its weakly bound, thin and platy nature (Fig. 10d). On Sol 881, a second mini-drill hole was created on a neighboring slab approximately 14–15 cm away from a new Mojave 2 full depth drill target. The Start Hole process took 4 cycles to reach a depth of 4.96 mm at Percussion Level 3 (Fig. 9a) and the Hardness Test increased the divot depth to 5.67 mm (Fig. 9b). The mini-drill penetrated the surface to a total depth of 19.88 mm in 50 s total drill-on time with a cumulative average rate of penetration of 0.238 mm/s at Percussion Levels 4 (0–10 & 30–50 s) and 5 (10–30 s) (Fig. 9c). These results also were comparable to those of the Confidence Hills target and the behavior of the mini-drill tailings was consistent with a dry granular powder (Fig. 10). Minor

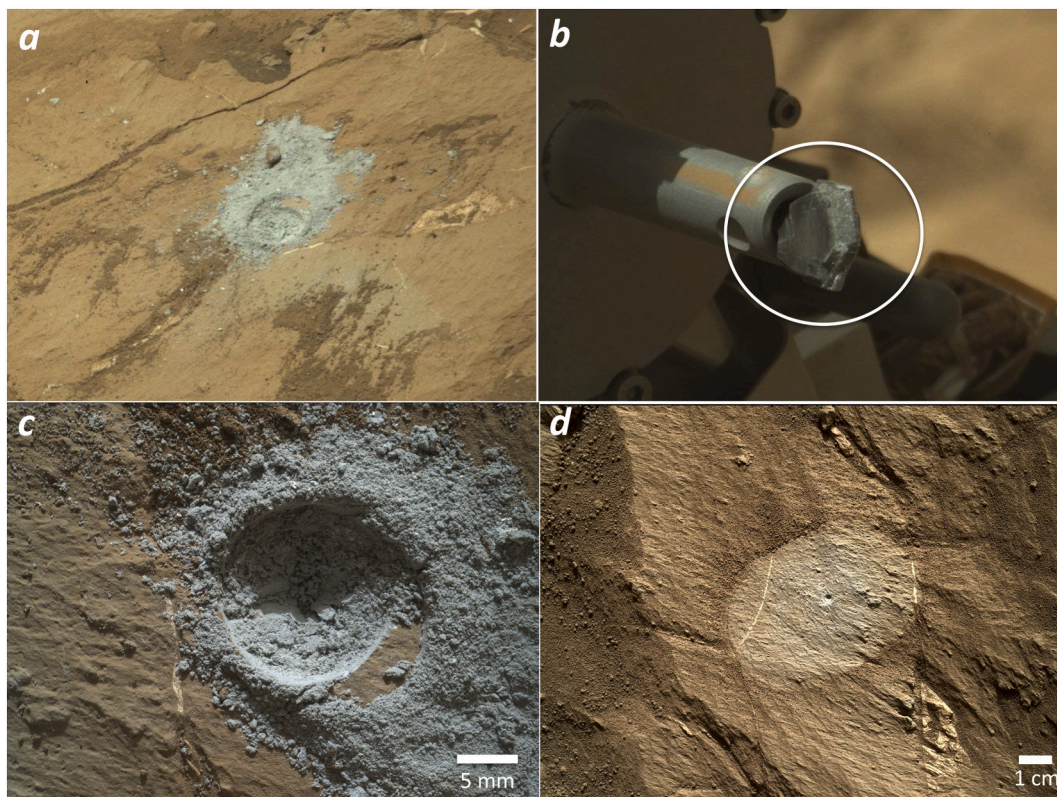


**Fig. 14.** Images from the Buckskin mini-start hole test acquired on Sol 1059 demonstrating that behavior of mini-start hole tailings is consistent with that of fine dry particulate material. (a) Mastcam image of tailings pile shows tailings flowing in downhill (run-off) direction (1059MR0046550010104694E01). (b) Mastcam image of drill bit after drilling (white circle) shows minimal amount of powder sticking to hardware (1059MR0046570000104690E01). (c) MAHLI image, taken from a standoff distance of 5 cm, shows ‘classic’ tailings pile and minor clumping disaggregating as tailings propagate toward the lower right corner of image (1059MH0005090000400393R00). (d) MAHLI image of DRT spot taken at a standoff distance of 25 cm on Sol 1057 (1057MH0001900010400301C00). Scratches near center of spot suggest that Murray formation is a relatively soft unit (compare to Fig. 17d). Note in all images drill bit and drill holes are 1.6 cm in diameter. *Image Credit:* NASA/JPL-Caltech/MSSS.

fractures did occur during this second test as well, but were less severe and the slab maintained its integrity throughout drilling. In addition, this would be the first target drilled using the new reduced percussion algorithm, which gave us the best chance of mitigating the risk of breaking the slab.

On Sol 882 the team commenced with full depth drilling and caching of the Mojave 2 sample using the reduced percussion protocol (Fig. 11). The Start Hole process took 6 cycles to reach a depth of 4.88 mm at Percussion Levels 1 (cycles 1–4) and 3 (cycles 5 & 6) (Fig. 9a). Note that a Hardness Test was not performed, as this is precluded by the new reduced percussion protocol. The full drill penetrated the surface to a maximum total depth of 65.04 mm in 590 s total drill-on time with a cumulative average rate of penetration of 0.099 mm/s and a maximum Percussion Level of 3 (Figs. 9c & 12). On Sol 884 the sample was transferred from the DBA to CHIMRA and into the scoop where it was visually estimated that  $12 \pm 2 \text{ cm}^3$  of material had been collected (Fig. 11d). The sample was then processed through the  $150 \mu\text{m}$  sieve path and a portion was delivered to CheMin on the same sol. Subsequently, three portions were delivered to SAM on Sol 892. Like the sample at Confidence Hills, CheMin results showed Mojave 2 is rich in pyroxene, phyllosilicates and hematite, with minor amounts of magnetite, apatite and jarosite (Rampe et al., 2017a). However, Mojave 2 is more abundant in jarosite ( $\sim 3.1 \text{ wt}\%$ ) than Confidence Hills. Jarosite is a K-rich sulfate and, as such, is a good candidate for K-Ar dating using SAM. A previous successful attempt with this method yielded an age of  $\sim 4.21 \text{ Ga}$  for the Cumberland sample (Farley et al., 2014); while an attempt on Windjana yielded an unreasonably young and unrepeatable age, probably due to its coarser grain size (Vasconcelos et al., 2016).

Martin et al. (2017) attempted to use this technique on the jarosite in the Mojave 2 sample. This yielded an upper age of  $4.07 \pm 0.63 \text{ Ga}$ , most likely from detrital plagioclase, and a lower age of  $2.12 \pm 0.36 \text{ Ga}$ , most likely associated with jarosite formation and mixing with K-bearing evaporites and/or phyllosilicates. While this younger number is complicated by potential loss of Ar after mineral formation, it still suggests post-depositional fluid flow at a time well after most surface fluvial activity had ceased on Mars.

#### 4.1.3. Telegraph peak

Telegraph Peak was the site selected for the final Pahrump Hills full depth drill target. It is about 7–8 m up section from where the Mojave 2 sample was collected (Fig. 4). At this site it proved challenging to find suitable targets for the DRT, mini-drill testing, and full depth drilling. However, the bulk chemical composition of the rock, as determined by ChemCam and APXS, suggested it was similar in chemistry and mineralogy to the rest of the Pahrump Hills samples, so it was recommended that mini-drill testing be skipped and that the team proceed directly to full depth drilling as long as the full depth drill tailings could be observed prior to transfer into CHIMRA. On Sol 908 the team commenced with full depth drilling and caching of the Telegraph Peak sample using the reduced percussion protocol (Fig. 13). The Start Hole process took 6 cycles to reach a depth of 5.50 mm at Percussion Level 1 (Fig. 9a). The full drill penetrated the surface to a maximum total depth of 65.86 mm in 662 s total drill-on time with a cumulative average rate of penetration of 0.090 mm/s and a maximum Percussion Level of 3 (Figs. 9c & 12). The resulting drill tailings were observed to be consistent with a dry granular powder, but the drill fault error on Sol 911 (see

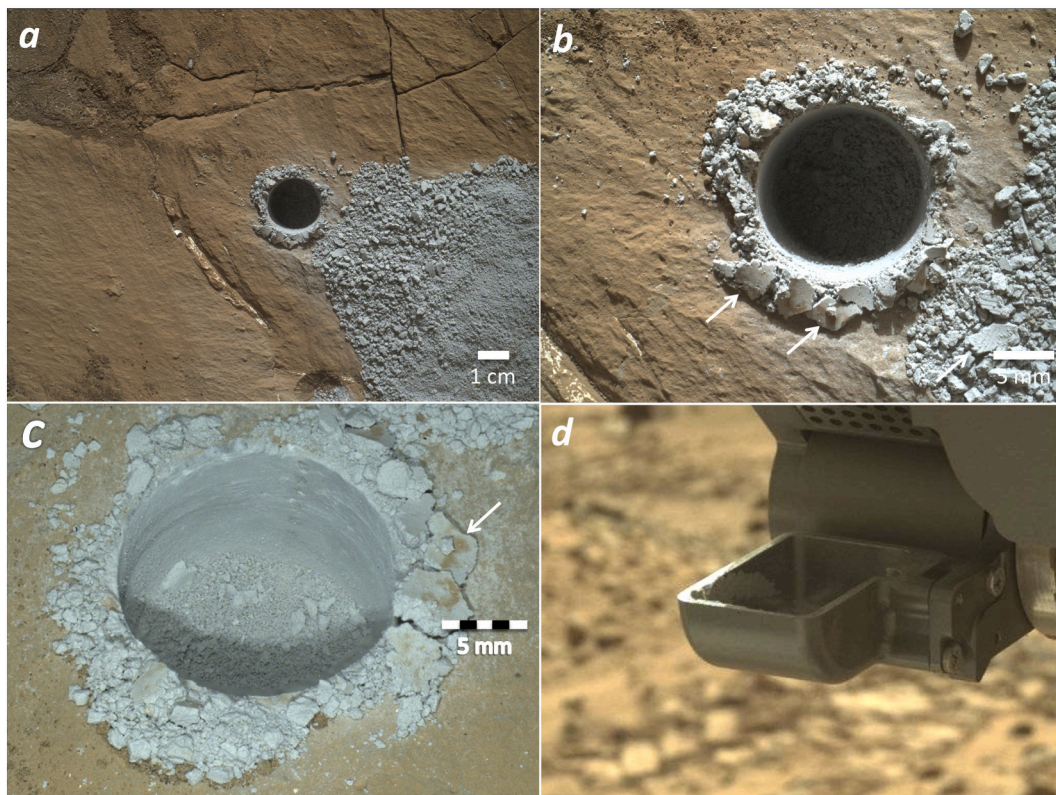


**Fig. 15.** Images from the Buckskin full depth drill campaign. (a) MAHLI image of both full depth drill hole (center) and mini-start hole (bottom edge; half cut-off) taken at a standoff distance of 25 cm on Sol 1060 (1060MH0003970010400402C00). (b) MAHLI image of full depth drill hole taken at a standoff distance of 5 cm on Sol 1060 (1065MH0005120000400729R00). Smooth-surfaced clumps (white arrows) likely formed via temporary cohesion to smooth surfaces on DBA. (c) MAHLI image of full depth drill hole taken at an oblique angle on Sol 1064 showing brown material (white arrow) adhering to surface of smooth clumps, likely dust previously coating surface of DBA (1065MH0005100000400593R00). Also seen, a vertical array of pits against the back wall of the hole created by the ChemCam laser. Image acquired at night under white light LED illumination. (d) Mastcam image of processed sample in scoop acquired on Sol 1061 (1061ML0046670000306182E01). Unfortunately, sample is below the rim of the scoop and unviewable, making volume estimate indeterminate. Note in all images drill hole is 1.6 cm in diameter. Scoop is 4.5 cm wide. *Image Credit:* NASA/JPL-Caltech/MSSS. (For interpretation of the references to color in this figure legend, the reader is referred to the web version of this article.)

above) delayed transfer of the sample from the DBA to CHIMRA until Sol 922. The sample was then moved to the scoop for inspection where it was estimated that  $18.8 \pm 1.3/-0.3 \text{ cm}^3$  of material had been collected based on CAD models; however, given the occlusion of the sample by the rim of the scoop, this is likely an overestimate (Fig. 13d). The sample was then processed through the  $150 \mu\text{m}$  sieve path and a portion was delivered to CheMin on the same sol. Subsequently, a portion was delivered to SAM on Sol 928 followed by three additional portions on Sol 954. CheMin results showed that Telegraph Peak is rich in magnetite, cristobalite and opal-CT, with minor amounts of jarosite and hematite, but no phyllosilicates (Rampe et al., 2017a). The greater concentration of magnetite in these rocks suggests they may have formed under more reducing conditions than those lower down in the Murray formation. Taken as a whole the mudstones at Pahrump Hills exhibit oxidizing (hematite), acidic (jarosite), reducing (magnetite), and alkaline (apatite and phyllosilicates) mineralogies. SAM analyses also provided additional evidence of this complicated geochemical history as indicated by the presence of oxidizing (nitrate, sulfate, and oxychlorine), and alkaline (carbonate) phases, along with evidence of organics (Sutter et al., 2017a). The mudstones of the lower Murray formation (including Buckskin below) appear to have been deposited in a lacustrine environment that records a complex pH and/or Eh history that may include deposition into lake waters under variable redox conditions, formation in a stratified lake where redox conditions were depth dependent, and/or post depositional diagenesis caused by multiple influxes of acidic pore

fluids (Hurowitz et al., 2017; Rampe et al., 2017a).

## 4.2. Marias Pass (Martian year 2)

### 4.2.1. Buckskin

Buckskin was the seventh rock drilled successfully on Mars and the fourth full depth drill hole drilled into the Murray formation. It is located in Marias Pass about 6 m up section from Telegraph Peak at Pahrump Hills (Fig. 4). Based on bulk chemical analysis by ChemCam and APXS, it was determined that this rock has elevated levels of Si ( $\text{SiO}_2$  62–68 wt%) compared to other rocks of the Murray formation. There was a great deal of interest in sampling a target with elevated Si, as high Si samples have a greater potential to preserve biosignatures (e.g., chert as described in Cady et al., 2003). In addition, elevated Si is highly suggestive of post-depositional fluid-rock interactions and may give us insight into the local aqueous history and the potential habitability of the region. Extensive ChemCam and APXS analyses demonstrated a distribution of Si contents across the Buckskin area, with some exhibiting higher Si than the Buckskin target itself (Frydenvang et al., 2017). Nonetheless, Buckskin would be the highest Si rock to be sampled thus far by full depth drilling. On Sol 1059 a mini-start hole was created approximately 6 cm away from the proposed Buckskin full depth drill target. This was the first time the mini-start hole process was used lieu of the mini-drill test. The mini-start hole process took 3 cycles to reach a depth of 3.20 mm at Percussion Level 3 (Fig. 9a). The Hardness Test increased the

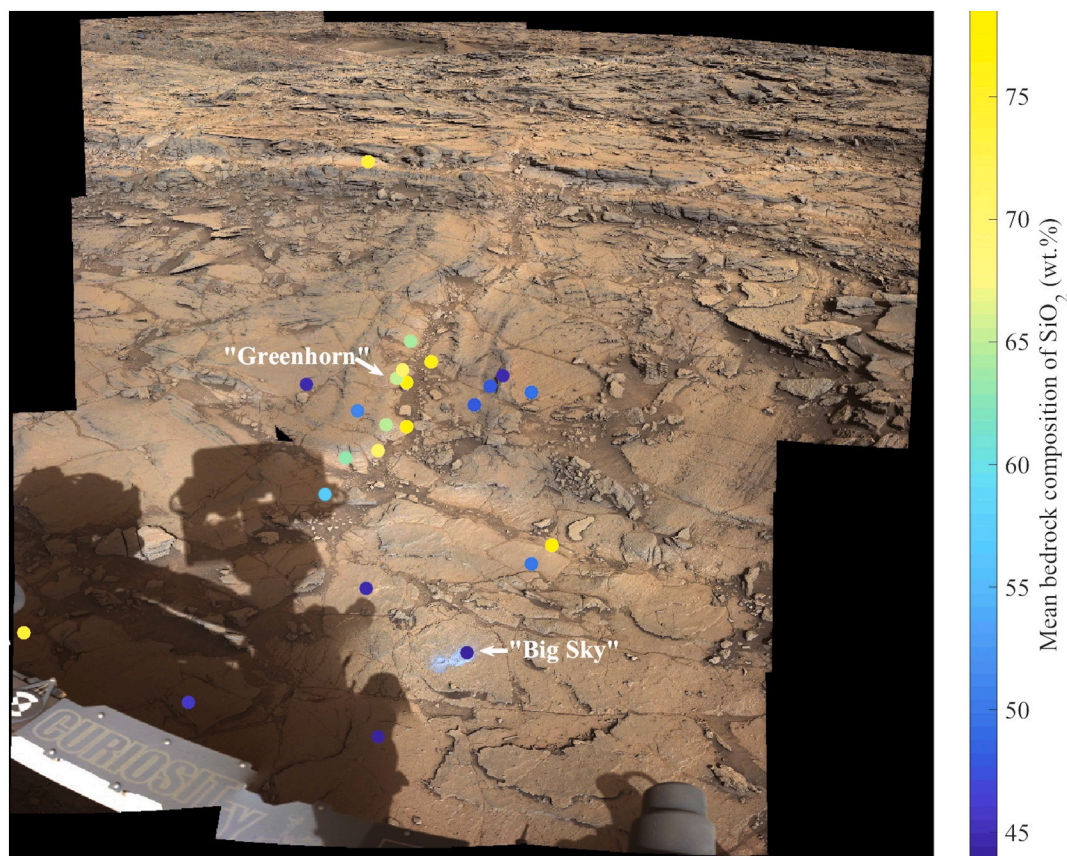


**Fig. 16.** Mastcam mosaic showing the location of the Big Sky and Greenhorn full depth drill targets relative to a light-toned alteration halo surrounding the prominent fracture in the center of the image. The alteration halo was characterized by increasing Si content closer to the core of the fracture zone. This is shown by the color coded dots, colors corresponding to the mean bedrock composition of SiO<sub>2</sub> (wt%), as determined by ChemCam, and denoted in the bar at right. The Big Sky target was chosen to represent more typical, less altered, Stimson sandstone, and as such is further away from the fracture, while the Greenhorn target was chosen to represent the more altered sandstone near the core of the fracture zone. For scale the Big Sky drill hole is 1.6 cm in diameter, and the two drill sites are ~2 m apart. This mosaic is composed of Mastcam images acquired between Sols 1112 and 1126 (PIA20270); note this is prior to the drilling of the Greenhorn target on Sol 1137. *Image Credit:* NASA/JPL-Caltech/MSSS.

divot depth by 0.90 mm to a total of 4.10 mm (Fig. 9b). The behavior of the mini-start hole tailings was consistent with that of fine, dry particulate material, giving the team confidence that this material would not pose a risk to flight hardware if ingested (Fig. 14). Also, experience at Pahrump Hills on similar Murray formation targets gave us additional confidence in this assessment. Enrichment in Si did not pose any additional concerns for the team.

On Sol 1060 the team commenced with full depth drilling and caching of the Buckskin sample using the reduced percussion protocol (Fig. 15). The Start Hole process took 7 cycles to reach a depth of 6.43 mm at Percussion Levels 1 (cycles 1–5) and 3 (cycles 6 & 7) (Fig. 9a). The full drill penetrated the surface to a maximum total depth of 64.50 mm in 680 s total drill-on time with a cumulative average rate of penetration 0.082 mm/s and a maximum Percussion Level of 3 (Figs. 9c & 12). On Sol 1061 the sample was transferred from the DBA to CHIMRA and into the scoop for inspection. Unfortunately, the sample was unviewable as it was almost entirely below the rim of the scoop, making the volume estimate indeterminate (Fig. 15d). The sample was then processed through the 150 μm sieve path and observed in the portion box where it was visually estimated that  $4 \pm 1$  cm<sup>3</sup> (sufficient for >50 portions) of material had passed through the sieve. A sample portion was then delivered to CheMin on the same sol and, subsequently, three portions were delivered to SAM on Sols 1075 and 1089.

CheMin determined that Buckskin has mineralogy similar to that of Telegraph Peak except with no jarosite or hematite and with abundant amorphous opaline silica and tridymite (~14 wt%). Tridymite is a low pressure, high temperature SiO<sub>2</sub> polymorph commonly associated on Earth with high-silica volcanism. This is the first time tridymite was identified on Mars and the first in situ mineralogic evidence for silicic Martian magmatism, hinting at the planet's complex petrogenetic history (i.e., Mars is more than just basalt) (Morris et al., 2016).

#### 4.3. Bridger Basin (Martian year 2)

Big Sky and Greenhorn were the eighth and ninth rocks successfully drilled on Mars. They are part of the Stimson formation and consist of well rounded, moderately well sorted fine-to-coarse-grained sandstones with local subrounded-to-subangular pebble sized grains.

This formation is characterized by ~1 m thick cross-bedding separated by sub-horizontal bounding surfaces and composed of uniform thickness cross-lamination interpreted as wind-ripple strata (Banham et al., 2018). It unconformably overlies deposits of the Murray formation. The science team had a strong desire to drill the Stimson as to date only one other sandstone (Windjana) had been previously drilled (Abbey et al., 2019). Also, Windjana was notably enriched in K (Treiman et al., 2016) and it was unclear whether it was representative of other

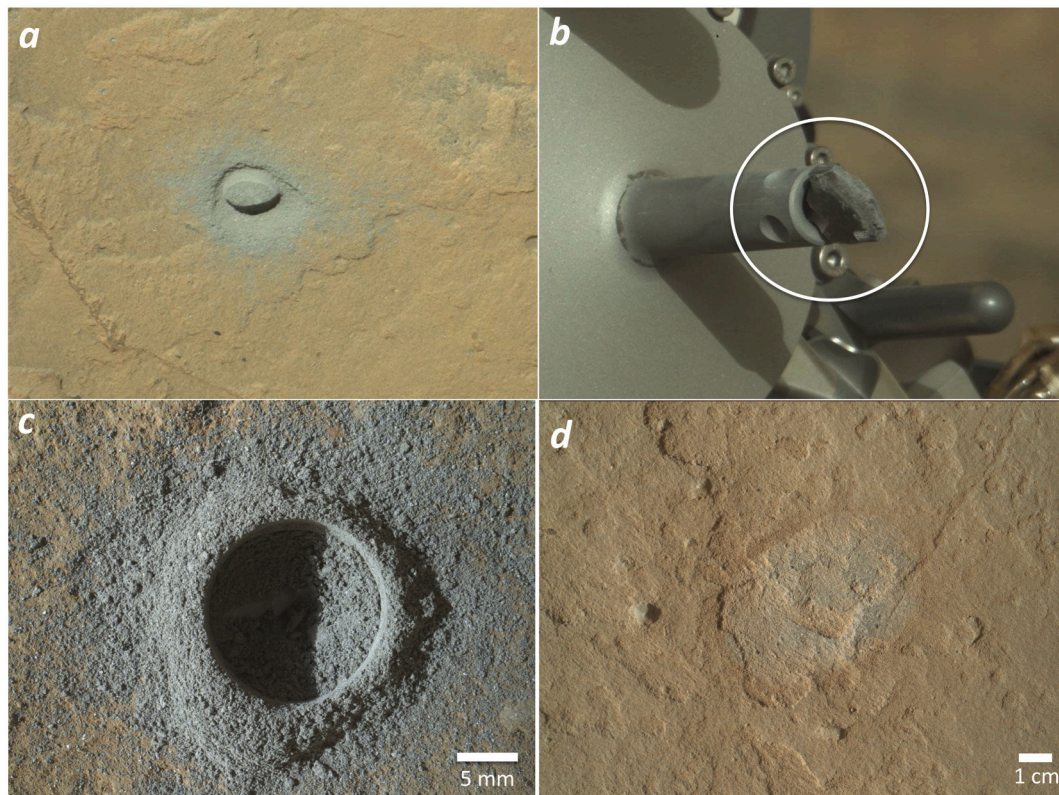


**Fig. 17.** Images from the Big Sky mini-start hole test acquired on Sol 1116 demonstrating that behavior of mini-start hole tailings is consistent with that of fine dry particulate material. (a) Mastcam image shows ‘classic’ tailings pile similar to those formed under dry conditions (1116MR0049730010601364E01). Lack of tailings propagation suggests surface is relatively level and stable. Note the barely visible gray DRT spot to the right of the mini-start hole. (b) Mastcam image of drill bit after drilling (white circle) shows minimal amount of powder sticking to hardware (1116MR0049750000601365E01). (c) MAHLI image, taken from a standoff distance of 5 cm, shows ‘classic’ tailings pile without the clumping noted in previous mini-start hole and mini-drill hole tests, most likely due to slightly coarser grain size of particulate material (1117MH0005090000401449R00). (d) MAHLI image of the barely visible DRT spot taken at a standoff distance of 25 cm on Sol 1114, suggesting the Stimson formation is more resistant than the Murray formation (1114MH0001900010401362C00) (compare to Fig. 14d). Note in all images drill bit and drill holes are 1.6 cm in diameter. *Image Credit:* NASA/JPL-Caltech/MSSS.

sandstones found in Gale crater. Bridger Basin was an ideal location to drill into Stimson sandstone as it hosted prominent ridges of this unit and they could be placed in reasonably good context with the underlying Murray mudstones (Fig. 4). In addition, it had been noted that fractures in the Stimson formation were commonly associated with lighter-toned alteration halos, averaging ~50 cm wide, that exhibited elevated Si content, similar in abundance to that seen at Buckskin. The team decided to create two full depth drill holes into two Stimson targets in close proximity to each other, one in an altered zone associated with one of these fractures and one in a nearby outcrop of more typical, less altered, sandstone (Fig. 16). It was hoped that by drilling into the same sedimentary deposit, at two sites affected differently by fluid flow, insights into the processes leading to Si-enrichment could be better elucidated than by comparing rocks from two different depositional environments. With the exception of the locally elevated levels of Si, the bulk chemistry of these rocks, as determined by ChemCam and APXS, were consistent with basaltic-derived sediments.

#### 4.3.1. Big Sky

Big Sky was selected as the first Stimson sandstone target drilled because its bulk chemical characteristics are consistent with typical (non Si-enriched) Stimson ( $\text{SiO}_2$  ~42 wt%). It was also the first sandstone to

be drilled since Windjana in the Kimberley formation during the first Martian year. On Sol 1116 a mini-start hole was created approximately 7 cm away from the proposed Big Sky full depth drill target. The mini-start hole process took 4 cycles to reach a depth of 4.38 mm at Percussion Level 3 (Fig. 9a). The Hardness Test increased the divot depth by 0.34 mm to a total of 4.72 mm (Fig. 9b). While these numbers demonstrated that the Stimson sandstone was slightly more resistant to penetration than the Murray mudstones encountered at Pahrump Hills, this was not unexpected and still in family with previously drilled targets, suggesting that reduced percussion would be adequate for full depth drilling. Furthermore, the behavior of the mini-start hole tailings was consistent with that of fine, dry particulate material, giving the team the assurance it needed to go forward with full depth drilling (Fig. 17). On Sol 1119 the team commenced with full depth drilling and caching of the Big Sky sample using the reduced percussion protocol (Fig. 18). The Start Hole process took 7 cycles to reach a depth of 5.22 mm at Percussion Levels 1 (cycles 1–4) and 3 (cycles 5–7) (Fig. 9a). The full drill penetrated the surface to a maximum total depth of 64.40 mm in 724 s total drill-on time with a cumulative average rate of penetration of 0.080 mm/s and a maximum Percussion Level of 4 (Figs. 9c & 12). On Sol 1121 the sample was transferred from the DBA to CHIMRA and into the scoop for inspection. Unfortunately, most of the sample was below

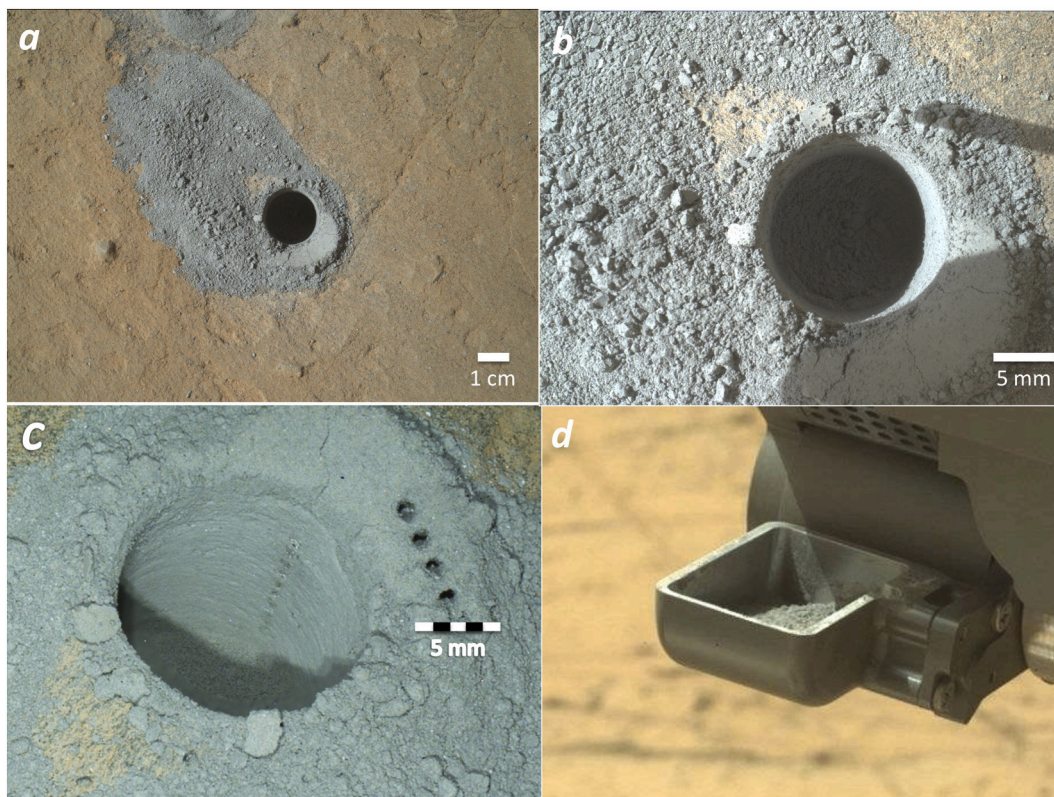


**Fig. 18.** Images from the Big Sky full depth drill campaign. (a) MAHLI image of full depth drill hole taken at a standoff distance of 25 cm on Sol 1119 (1119MH0003970010401458C00). (b) MAHLI image of full depth drill hole taken at a standoff distance of 5 cm on Sol 1119 (1119MH0004230000401503R00). (c) MAHLI image of full depth drill hole taken from an oblique angle on Sol 1123 (1124MH0005240000401685R00). A vertical array of pits against the back wall of the hole and a horizontal array of pits in the tailings can be seen created by the ChemCam laser. Image acquired at night under white light LED illumination. (d) Mastcam image of processed sample in scoop acquired on Sol 1121 (1121ML0049950000501158E01). Note in all images drill hole is 1.6 cm in diameter. Scoop is 4.5 cm wide. *Image Credit:* NASA/JPL-Caltech/MSSS.

the rim of the scoop, making the volume estimate indeterminate, though it appeared to be in family with previous samples (Fig. 18d). The sample was then processed through the 150  $\mu\text{m}$  sieve path and observed in the portion box where it was visually estimated that  $7.5 \pm 1 \text{ cm}^3$  of material had passed through the sieve. A sample portion was then delivered to CheMin on the same sol and, subsequently, three portions were delivered to SAM on Sol 1129. As expected, CheMin determined that Big Sky has an overall mineralogy dominated by plagioclase feldspar and pyroxene, consistent with sediments derived from basaltic source material, and likely formed under neutral or moderate pH conditions (pH  $\sim$ 6–8) (Hausrath et al., 2017). Furthermore, APXS confirmed that its elemental composition was similar to that of average Martian soil (Yen et al., 2017).

#### 4.3.2. Greenhorn

Greenhorn was the second Stimson sandstone target drilled because of its occurrence within the light-toned alteration halo of a prominent fracture zone and its proximity to Big Sky, approximately 2 m away. While its Si content was not as high as the team would have preferred ( $\text{SiO}_2 \sim 56 \text{ wt}\%$ ), targets with higher Si values ( $\text{SiO}_2 > 70 \text{ wt}\%$ ) proved difficult for the rover arm to reach. In addition, Greenhorn exhibited similar chemical trends as these higher Si rocks (Al vs Ti, Ti vs Si, etc.), suggesting it may represent the transition from unaltered to altered

sandstone, so it was decided it would be worthwhile to collect a full depth drill sample. However, one point of concern was that sulfur levels, as determined by APXS, were elevated beyond that of any rocks drilled up to this point ( $\sim 11 \text{ wt}\%$ ), raising the possibility that Fe-sulfates were present which could potentially clog up the sampling system. This threat was deemed unlikely though, as iron levels in Greenhorn were not particularly high ( $< 10 \text{ wt}\%$ ). So, on Sol 1134 a mini-start hole on a pre-existing contact science target called ‘Pilgrim’ was created approximately 40 cm away from the proposed Greenhorn full depth drill target. The mini-start hole process took 4 cycles to reach a depth of 4.49 mm at Percussion Level 3 (Fig. 9a). The Hardness Test increased the divot depth by 0.64 mm to a total of 5.13 mm (Fig. 9b). These results were comparable to the Big Sky target and the behavior of the mini-start hole tailings was consistent with that of fine, dry particulate material, giving the team the assurance it needed to go forward with full depth drilling (Fig. 19). On Sol 1137 the team commenced with full depth drilling and caching of the Greenhorn sample using the reduced percussion protocol (Fig. 20). The Start Hole process took 7 cycles to reach a depth of 4.77 mm at Percussion Levels 1 (cycles 1–4) and 3 (cycles 5–7) (Fig. 9a). The full drill penetrated the surface to a maximum total depth of 65.32 mm in 710 s total drill-on time with a cumulative average rate of penetration of 0.084 mm/s and a maximum Percussion Level of 4 (Figs. 9c & 12). On Sol 1139 the sample was transferred from the DBA to CHIMRA and into

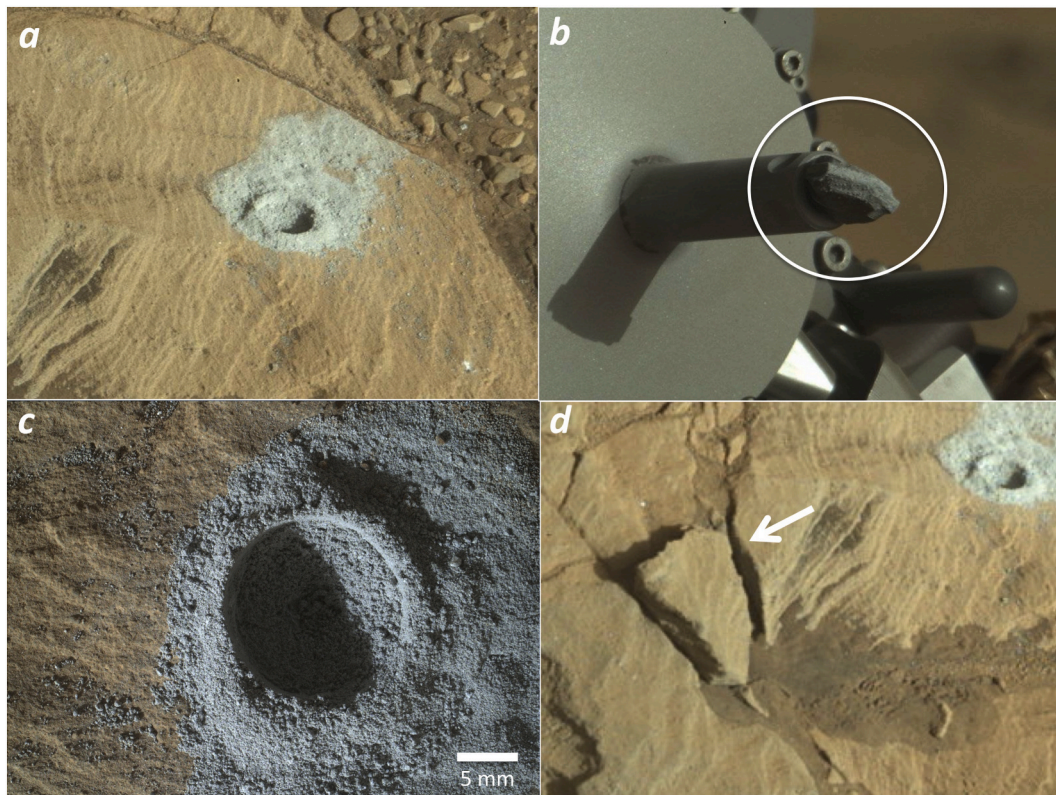


**Fig. 19.** Images from the Pilgrim mini-start hole test acquired on Sol 1134 demonstrating that behavior of mini-start hole tailings is consistent with that of fine dry particulate material. (a) Mastcam image shows ‘classic’ tailings pile and tailings flowing over pre-existing topography (1134MR0050650010601602E01). (b) Mastcam image of drill bit after drilling (white circle) shows minimal amount of powder sticking to hardware (1134MR0050680000601605E01). (c) MAHLI image, taken from a standoff distance of 5 cm, shows ‘classic’ tailings pile and minimal clumping, most likely due to size of particulate material, similar to that seen at Big Sky (1134MH0005090000401946R00). (d) Mastcam showing block ( $\sim 3 \times 5$  cm) dislodged as a result of mini-start hole percussion (white arrow) (1134MR0050660010601604E01). Note in all images drill bit and drill holes are 1.6 cm in diameter. *Image Credit:* NASA/JPL-Caltech/MSSS.

the scoop where it was estimated that  $28.8 + 1.3/-0.3 \text{ cm}^3$  of material had been collected based on CAD models; however, given the occlusion of the sample by the rim of the scoop, this is likely an overestimate (Fig. 20d). The sample was then processed through the  $150 \mu\text{m}$  sieve path and a portion was delivered to CheMin on the same sol. Subsequently, three portions were delivered to SAM on Sols 1147 and 1178. CheMin determined that, like Big Sky, Greenhorn is dominated by plagioclase feldspar and pyroxene, however, the amount of  $\text{SiO}_2$ -enriched amorphous material present in Greenhorn is 2–3 times higher than that present in Big Sky. This marked increase in  $\text{SiO}_2$ , along with a corresponding decrease in total FeO,  $\text{Al}_2\text{O}_3$  and MgO, is suggestive of alteration by acidic fluids ( $\text{pH} < 4$ ). This interpretation is consistent with the much higher concentration of Ca-sulfate minerals in Greenhorn ( $\sim 20 \text{ wt}\%$ ) when compared to the unaltered Big Sky sample ( $\sim 1.5 \text{ wt}\%$ ) (Hausrath et al., 2017; Yen et al., 2017). However, the amount of  $\text{SiO}_2$  present in Greenhorn is much higher ( $\sim 10 \text{ wt}\%$ ) than would be predicted by acid leaching alone, suggesting a natural evolution of fluid chemistry to more neutral or alkaline conditions where  $\text{SiO}_2$  is more soluble ( $\text{pH} > 9$ ). Further evidence of less acidic conditions was the detection by SAM of carbonate in the Greenhorn sample, but not in Big Sky, at levels below the detection limit of CheMin ( $\sim 1 \text{ wt}\%$ ) (Frydenvang et al., 2017; Yen et al., 2017).

#### 4.4. Naukluft Plateau (Martian year 2)

Lubango and Okoruso were the tenth and eleventh rocks successfully drilled on Mars and the third and fourth full depth drill holes drilled into the Stimson formation. They were located on the Naukluft Plateau only about 5 m up section from Big Sky and Greenhorn (Fig. 4). At this new location there was a strong desire to repeat the Big Sky-Greenhorn experiment in order to better constrain the alteration process(es) responsible for the observed chemical and mineralogical variation noted at Bridger Basin. This was especially important as the fracture-associated alteration halos are among the youngest features identified at Gale crater and understanding this fracture/alteration process could put important constraints on the fluid history of the crater (Frydenvang et al., 2017). In addition, this was the last chance during the mission to sample Stimson sandstone based on its mapped orbital extent (Stack et al., 2017) and the likely future path of the rover and there was a desire to establish a better baseline for the mineralogical variability of this unit. The bulk chemistry of these rocks, as determined by ChemCam and APXS, indicated that they are comparable to the Big Sky and Greenhorn targets, suggesting to the team that there was little danger to the rover hardware if drilling was attempted at this location.

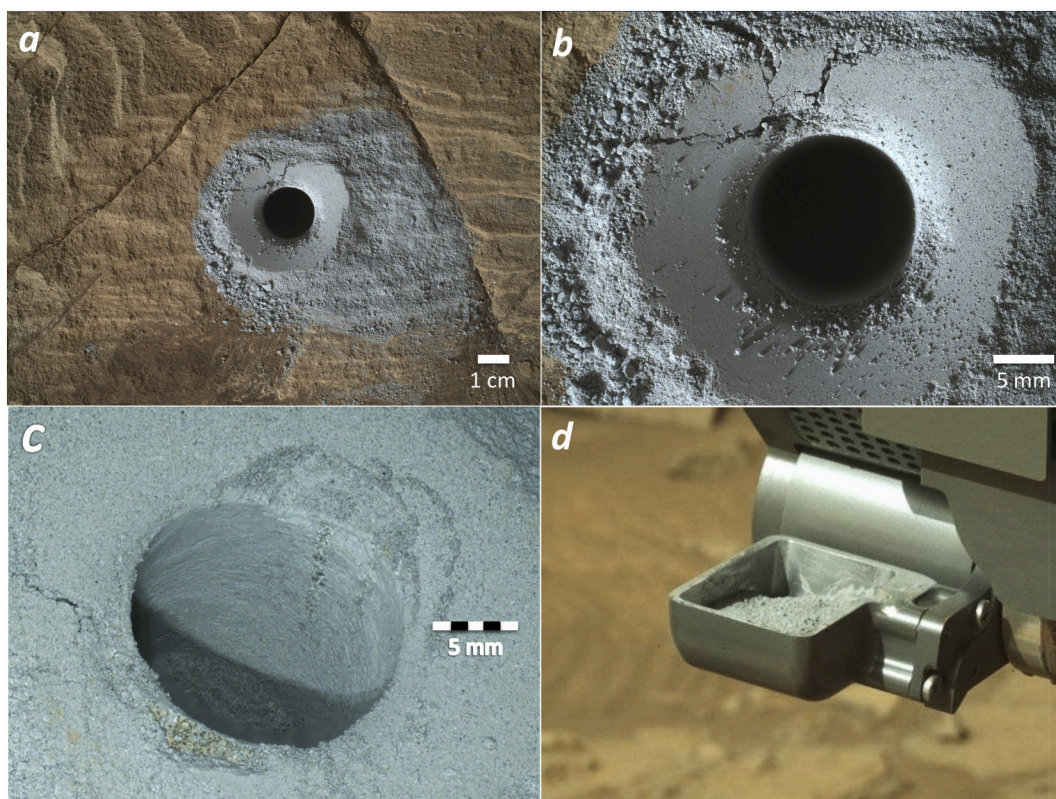


**Fig. 20.** Images from the Greenhorn full depth drill campaign. (a) MAHLI image of full depth drill hole taken at a standoff distance of 25 cm on Sol 1137 (1137MH0003970010401960C00). (b) MAHLI image of full depth drill hole taken at a standoff distance of 5 cm on Sol 1137 (1138MH0004230000402005R00). (c) MAHLI image of full depth drill hole taken from an oblique angle on Sol 1142 (1142MH0005310000402151R00). Two vertical arrays of pits can just be seen against the back wall of the hole created by the ChemCam laser. Image acquired at night under white light LED illumination. (d) Mastcam image of processed sample in scoop acquired on Sol 1139 (1139ML0051510000501390E01). Note in all images drill hole is 1.6 cm in diameter. Scoop is 4.5 cm wide. *Image Credit:* NASA/JPL-Caltech/MSSS.

#### 4.4.1. Lubango

Lubango was selected to be the third Stimson sandstone target drilled because of its occurrence within the light-toned alteration halo of a prominent fracture zone. While its Si content was not as high as the team would have preferred ( $\text{SiO}_2 \sim 58 \text{ wt}\%$ ), it was at least comparable to that of the high Si Greenhorn target. Furthermore, this data was acquired using APXS about 6 cm away from the core of the fracture zone, in order to accommodate the DRT prior to analysis, and ChemCam data suggested that Si content increased as one approached the core of the fracture zone, averaging  $\sim 73 \text{ wt}\%$  (with a high  $>90 \text{ wt}\%$ ) at a distance of 2–2.5 cm from the edge of the core, the proposed site of the full depth drill target. So there was every hope that any sample acquired would be more enriched in Si than indicated by the APXS measurement. However, one major point of concern was drilling so close to the rock face that defined the core of the fracture zone (Fig. 21). This significantly increased the chance of breaking the rock during full depth drilling. While this did not pose any risk to the rover hardware as demonstrated from the Bonanza King ‘successful failure’ sample, it did pose a risk to science. If the borehole fractured, sample would be lost, but given the importance to the science team of collecting the highest Si sample possible at this location, the risk of drilling close to the fracture face was deemed necessary and unavoidable. The bulk chemical composition of the rock suggested it was similar in chemistry and mineralogy to Stimson samples acquired at Bridger Basin and was expected to behave in family with those recent drill targets. Due to the small amount of workspace available at this site, it was recommended that both the mini-drill test and the mini-start hole procedure be skipped and that the team could proceed directly to full depth drilling. On Sol 1320 the team commenced with full depth drilling and caching of the Lubango sample using the

reduced percussion protocol (Fig. 22). The Start Hole process took 7 cycles to reach a depth of 5.22 mm at Percussion Levels 1 (cycles 1–4) and 3 (cycles 5–7) (Fig. 9a). The full drill penetrated the surface to a maximum total depth of 65.27 mm in 770 s total drill-on time with a cumulative average rate of penetration of 0.076 mm/s and a maximum Percussion Level of 4 (Figs. 9c & 12). On Sol 1323 the sample was transferred from the DBA to CHIMRA and into the scoop where it was estimated that  $11.7 + 1.3 / -0.3 \text{ cm}^3$  of material had been collected based on CAD models (Fig. 22d). The sample was then processed through the 150  $\mu\text{m}$  sieve path and a portion was delivered to CheMin on the same sol. No SAM analysis was performed on this sample. CheMin determined that Lubango, like Greenhorn, shows a marked increase in  $\text{SiO}_2$ -enriched amorphous material compared to unaltered Stimson, as well as an increase in Ca-sulfate content, suggesting that it too was subjected to alteration by acidic fluids. However, like Greenhorn, the amount of  $\text{SiO}_2$  present is in excess ( $\sim 6 \text{ wt}\%$ ) of that expected if acid leaching was the sole cause of alteration, further suggesting an evolution of water chemistry to more neutral or alkaline conditions. The concentration of Ca-sulfate minerals in Lubango ( $\sim 24 \text{ wt}\%$ ) is also consistent with an initial pulse of acidic alteration when compared to the less altered Okoruso sample ( $\sim 2 \text{ wt}\%$ ) described below (Yen et al., 2017). It should also be noted that this analysis included the first ever direct detection of three different hydration states of Ca-sulfate in a single sample, as well as the first ever in situ detection of gypsum on Mars (Vaniman et al., 2017).

#### 4.4.2. Okoruso

Okoruso was the fourth Stimson sandstone target drilled because its bulk chemical characteristics are consistent with typical (non-Si-

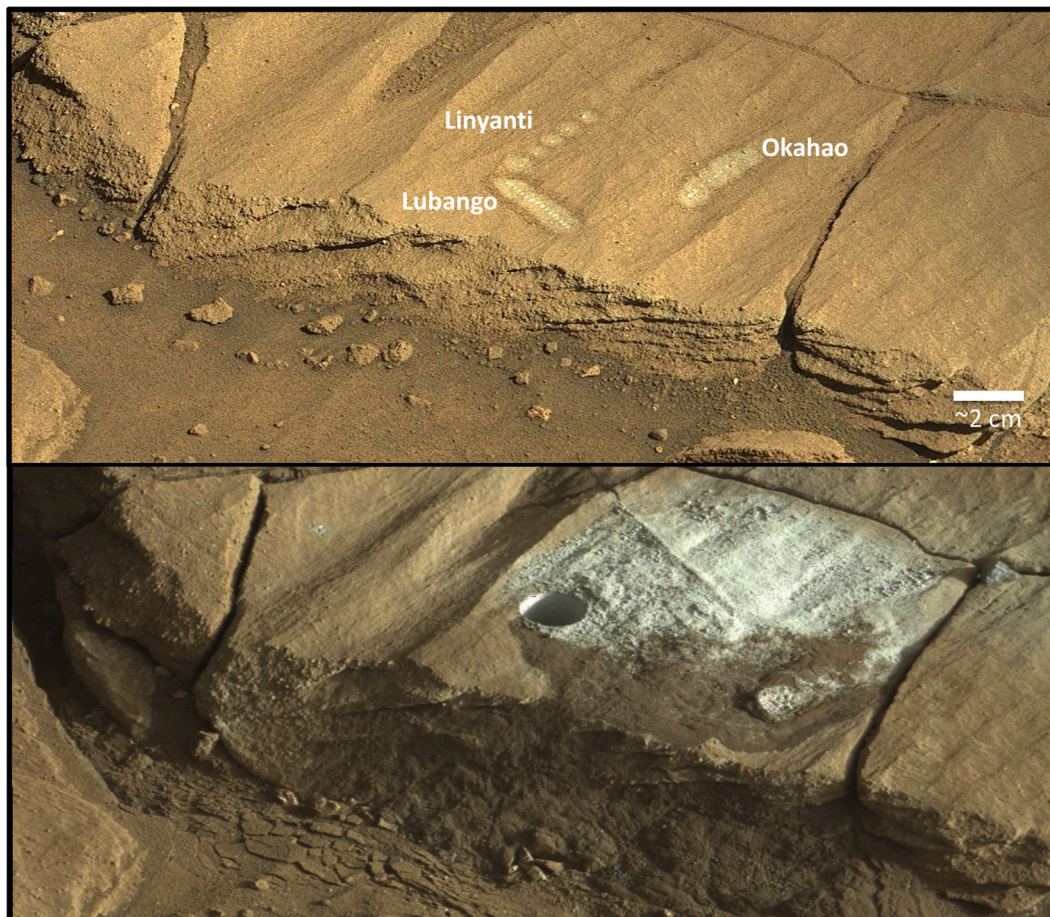


**Fig. 21.** Mastcam images taken on Sols 1317 (top) and 1321 (bottom), showing the Lubango target before and after full depth drilling (1317MR0062830010700571E01 & 1321MR0063120010700632E01). ChemCam data suggested that the Si content increased closer to the fracture edge: Okahao, average  $\text{SiO}_2$  ~64 wt% (highest >70 wt%); Linyanti, average  $\text{SiO}_2$  ~75 wt% (highest >80 wt%); Lubango, average  $\text{SiO}_2$  ~73 wt% (highest >90 wt%). Drilling at Lubango, a distance of only 2–2.5 cm from the fracture face, significantly increased the chance of breaking the rock during the full depth drill; however, this did not occur. *Image Credit:* NASA/JPL-Caltech/MSSS.

enriched) Stimson ( $\text{SiO}_2$  ~43 wt%) and are comparable to that of the unaltered Big Sky target. It also lies approximately 4.8 m away from Lubango. The bulk chemical composition of the rock suggested it was similar in chemistry and mineralogy to Stimson samples previously acquired and was expected to behave in family with those drill targets, so it was recommended that both the mini-drill test and the mini-start hole procedure be skipped and that the team proceed directly to full depth drilling. However, one point of concern was loose debris above the full depth drill target that may be mobilized during drill percussion, but this was determined to pose little risk to the flight hardware, and due to the nature of sample collection (sample is moved up a collection tube in contact with the bore hole) there was little risk of contaminating any acquired sample, though this did mean that caution would need to be taken if drill tailings left on the surface were to be analyzed at a later date. Another point of concern was that the majority of the right rear wheel was not in contact with the ground, raising the possibility that the rover could suddenly slip by as much as 3 cm, but it was determined that the potential loads a wheel slip of this magnitude would put on the arm in its current pose could be tolerated without risk to either the arm or the drill system. In addition, there had been zero slip detected since the

rover had parked at this location several sols prior, thus the risk of wheel slip was deemed negligible. So, on Sol 1332 the team commenced with full depth drilling and caching of the Okoruso sample using the reduced percussion protocol (Fig. 23). The Start Hole process took 7 cycles to reach a depth of 4.95 mm at Percussion Levels 1 (cycles 1–4) and 3 (cycles 5–7) (Fig. 9a). The full drill penetrated the surface to a maximum total depth of 65.11 mm in 700 s total drill-on time with a cumulative average rate of penetration of 0.085 mm/s and a maximum Percussion Level of 3 (Figs. 9c & 12). On Sol 1334 the sample was transferred from the DBA to CHIMRA and into the scoop where it was estimated that  $6.2 + 1.3/-0.3 \text{ cm}^3$  of material had been collected based on CAD models (Fig. 23d). The sample was then processed through the 150  $\mu\text{m}$  sieve path and a portion was delivered to CheMin on the same sol. No SAM analysis was performed on this sample. CheMin determined that Okoruso, like Big Sky, has an overall mineralogy and elemental composition typical of unaltered Stimson. However, in combination with the observations made for Greenhorn and Lubango, a complicated diagenetic history of subsurface fluid flow, including multiple stages of aqueous alteration propagating along fractures under a variety of environmental conditions (e.g., both low and high pH), can be demonstrated for this

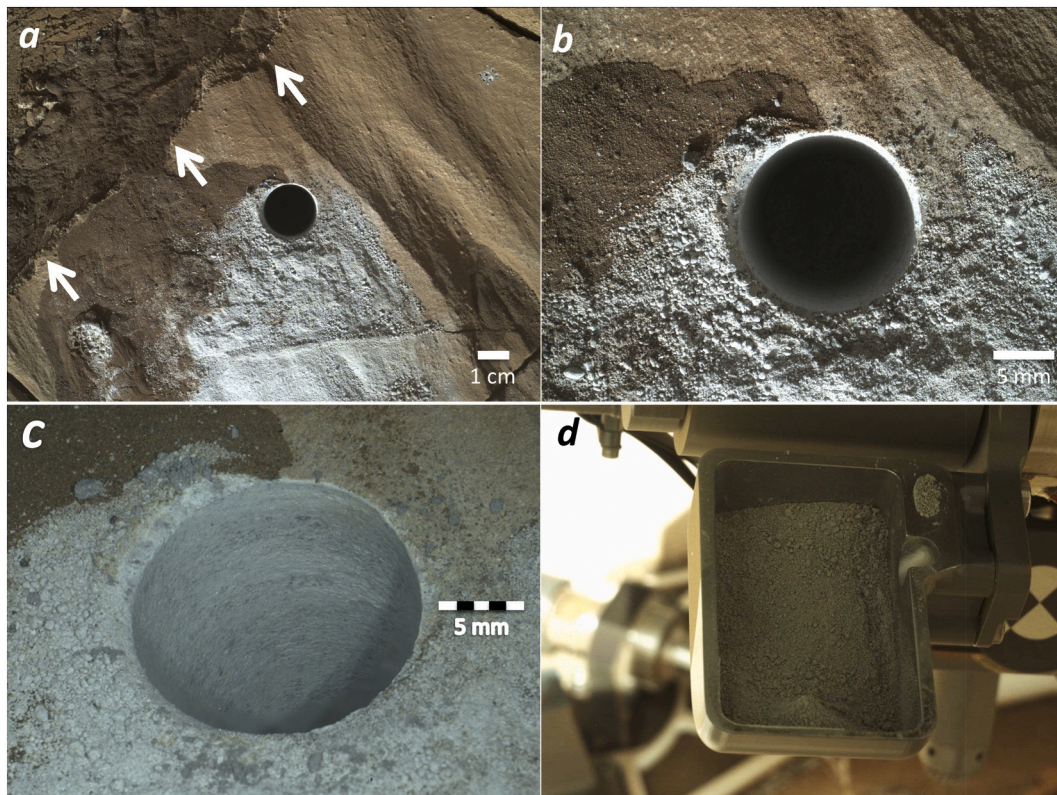


**Fig. 22.** Images from the Lubango full depth drill campaign. (a) MAHLI image of full depth drill hole taken at a standoff distance of 25 cm on Sol 1321 (1321MH0005920010500607C00). Note the darker toned fine dust emanating from the edge of the plate (i.e., the core of the fracture zone; white arrows), likely mobilized by drill percussion. (b) MAHLI image of full depth drill hole taken at a standoff distance of 5 cm on Sol 1321 (1321MH0004230000500656R00). (c) MAHLI image of full depth drill hole taken from an oblique angle on Sol 1324 (1325MH0005990000500810R00). Image acquired at night under white light LED illumination. (d) Mastcam image of processed sample in scoop acquired on Sol 1323 (1323ML0063170010406080E01). For this and subsequent inspection images, scoop poses were altered from previous targets to allow for more consistent sample observation and more accurate volume estimation. Note in all images drill hole is 1.6 cm in diameter. Scoop is 4.5 cm wide. *Image Credit:* NASA/JPL-Caltech/MSSS.

region of Gale crater (Frydenvang et al., 2017; Hausrath et al., 2017; Yen et al., 2017).

#### 4.5. West of Naukluft Plateau (Martian year 3)

##### 4.5.1. Oudam

Oudam was the twelfth rock drilled on Mars and the fifth full depth drill hole drilled into the Murray formation. It is located west of the Naukluft Plateau about 12 m in elevation above Buckskin, the last previously drilled Murray target in Marias Pass (Fig. 4). It had been identified from orbit as a member of a much brighter or lighter-toned band of Murray comprising a roughly 15 m thick, laterally traceable stratigraphic unit outcropping on lower Mt. Sharp. The suspicion was that this color change was indicative of enrichment in silica, a high sampling priority for the team. However, APXS analysis revealed that these rocks only contained silica levels slightly higher than that for typical Murray ( $\text{SiO}_2 \sim 53$  wt%) and did not approach the levels of higher silica targets such as Buckskin ( $\text{SiO}_2$  62–68 wt%). While locating a high Si target was still a priority for the team, it was decided that the best way to do this going forward was by initiating a systematic stratigraphic survey at regularly spaced intervals as the rover was about to begin a traverse up section through  $\sim 250$  m of Murray formation. In addition, all other Murray formation samples up to this point (and subsequently) had been (lacustrine?) mudstone, while Oudam appeared to be cross-stratified siltstone, potentially representing an aeolian or fluvial interval within the Murray formation. So it was decided that drilling at the current location would be a valuable reference point for the systematic drilling campaign planned for the upcoming traverse through the Murray

formation (e.g., Bristow et al., 2018). Since the bulk chemical composition of the rock, as determined by APXS and ChemCam, suggested it was similar in chemistry and mineralogy to previous Murray samples acquired at Pahrump Hills and Marias Pass, and was expected to behave in family with those drill targets, it was recommended that both the mini-drill test and the mini-start hole procedure be skipped and that the team proceed directly to full depth drilling.

On Sol 1361 the team commenced with full depth drilling and caching of the Oudam sample using the reduced percussion protocol (Fig. 24). The Start Hole process took 7 cycles to reach a depth of 5.34 mm at Percussion Levels 1 (cycles 1–4) and 3 (cycles 5–7) (Fig. 9a). The full drill penetrated the surface to a maximum total depth of 65.29 mm in 750 s total drill-on time with a cumulative average rate of penetration of 0.078 mm/s and a maximum Percussion Level of 4 (Figs. 9c & 12). On Sol 1362 the sample was transferred from the DBA to CHIMRA and into the scoop where it was estimated that  $6.2 \pm 1.3 / -0.3 \text{ cm}^3$  of material had been collected based on CAD models (Fig. 24d). The sample was then processed through the 150  $\mu\text{m}$  sieve path and portions were delivered to CheMin on the same sol and again on Sol 1375. Subsequently, a portion was delivered to SAM on Sol 1382, with three additional portions delivered to SAM on Sol 1409. CheMin determined that Oudam is similar to previous Murray samples from Pahrump Hills, enriched in pyroxene, phyllosilicates and hematite, but is also enriched in Ca-sulfate, and contains very little magnetite and no detectable jarosite (Rampe et al., 2017b). Significantly, this sample contains the most hematite observed on the mission up to this time and represents a dramatic shift in the diagenetic history of the Murray formation when compared to the more magnetite rich mudstones collected

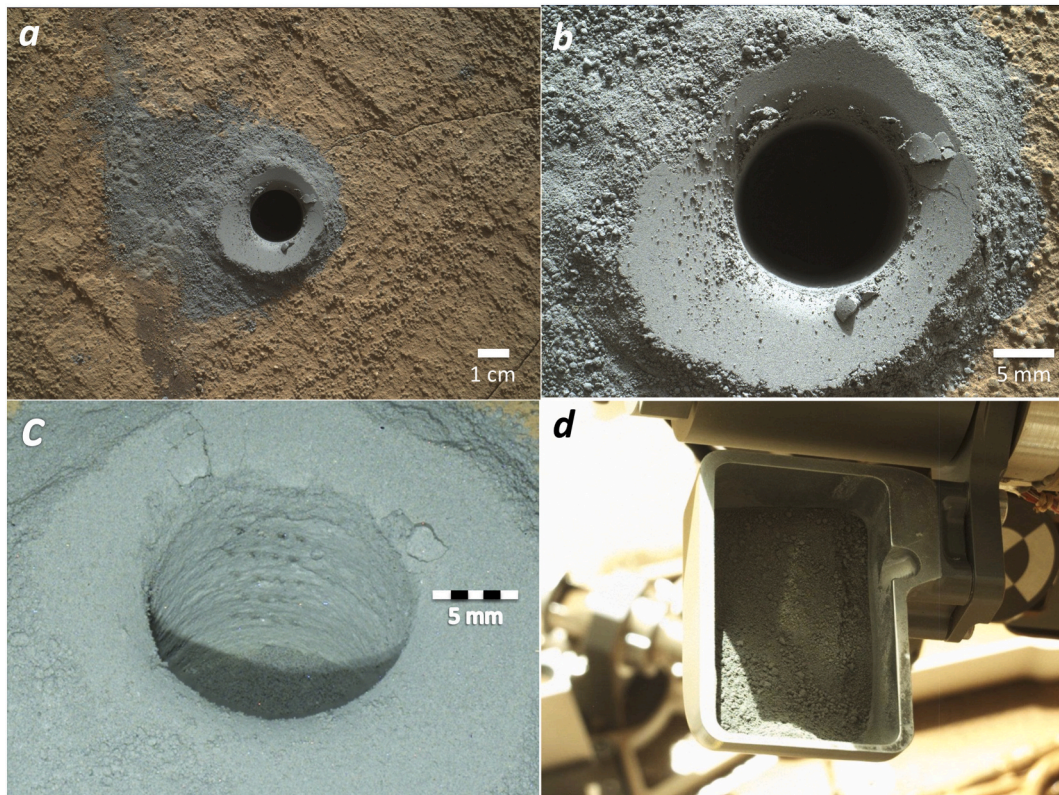


**Fig. 23.** Images from the Okoruso full depth drill campaign. (a) MAHLI image of full depth drill hole taken at a standoff distance of 25 cm on Sol 1332 (1332MH0005920010501230C00). (b) MAHLI image of full depth drill hole taken at a standoff distance of 5 cm on Sol 1332 (1332MH0004230000501279R00). (c) MAHLI image of full depth drill hole taken from an oblique angle on Sol 1337 (1338MH0005880000501506R00). A  $4 \times 5$  grid pattern of pits can be seen against the back wall of the hole created by the ChemCam laser. Image acquired at night under white light LED illumination. (d) Mastcam image of processed sample in scoop acquired on Sol 1334 using new and improved scoop poses (1334ML0064030010600101E01). Note in all images drill hole is 1.6 cm in diameter. Scoop is 4.5 cm wide. *Image Credit:* NASA/JPL-Caltech/MSSS.

lower down in the section (and at Yellowknife Bay). In addition, Calcifate appears to be present as a matrix component (as opposed to secondary vein material), also suggesting a major shift in the composition of diagenetic fluids affecting the Murray formation up section from Pahrump Hills (Bristow et al., 2018; Sutter et al., 2017b).

#### 4.6. Murray Buttes region (Martian year 3)

Marimba, Quela, and Sebina were the thirteenth, fourteenth, and fifteenth rocks successfully drilled on Mars and the sixth, seventh, and eighth full depth drill holes drilled into the Murray formation. They were located in the vicinity of Murray Buttes, an area comprised of abundant buttes and mesas capped by well layered, cross-stratified Stimson sandstone (Fig. 4). In this region there was a strong desire to continue the systematic sampling of the Murray formation at set intervals as the rover progressed up section toward Vera Rubin ridge (VRR, formerly called Hematite ridge), the next major geologic waypoint approximately 2 km away (Fraeman et al., 2020). Understanding the mineralogical heterogeneity of the Murray formation, and on what spatial/temporal scale it varies, would allow the team to better interpret the (variable?) petrogenesis of this formation, and help ground truth orbital data. In addition, up to this point, Curiosity had only sampled ~100 m of vertical section since Yellowknife Bay, and we had well over 150 m of vertical section to traverse before reaching the base of VRR. Also, understanding how the underlying Murray formation varies as it approached VRR would help the team better interpret this important transition. So it was decided that the rover would attempt to drill and collect sample every ~25 m of elevation, as permitted by terrain, viable

sampling location, etc., as it progressed up Mt. Sharp. To save time, the new baseline would be to deliver sample to CheMin only. However, sample would be cached in CHIMRA and could be delivered to SAM at a later date if CheMin results proved interesting.

##### 4.6.1. Marimba

Marimba was the sixth Murray mudstone target drilled. It is located 25–26 m up section from Oudam. Since its bulk chemistry as determined by APXS and ChemCam was determined to be similar to previously drilled Murray samples, it was decided that the team could proceed directly to full depth drilling without performing either the mini-start hole test or mini-drill hole procedure. So, on Sol 1420, the team commenced with full depth drilling and caching of the Marimba sample using the reduced percussion protocol. However, the Start Hole process only reached a depth of 4.00 mm after 10 cycles at Percussion Levels 1 (cycles 1–4) and 3 (cycles 5–10), timing out before exceeding the minimum required depth of 4.5 mm, which is typically reached after 4–7 cycles. There was no loss of preload during drilling indicating that neither the rock nor rover moved significantly during the attempt, the target simply proved to be more resistant in the first few millimeters than any previously drilled sample on Mars. The team decided that it was worth trying again, but that any attempt would likely only succeed if the Percussion Level was increased. However, ever since the drill fault error on Sol 911, percussion had been capped at Level 4 to help mitigate further degradation of the drill hardware. The team decided to allow the Start Hole procedure, normally limited to Percussion Level 3, to access Percussion Level 4, thereby increasing the chance of obtaining a sample, while respecting the limits placed on percussion usage. So, on Sol 1422,

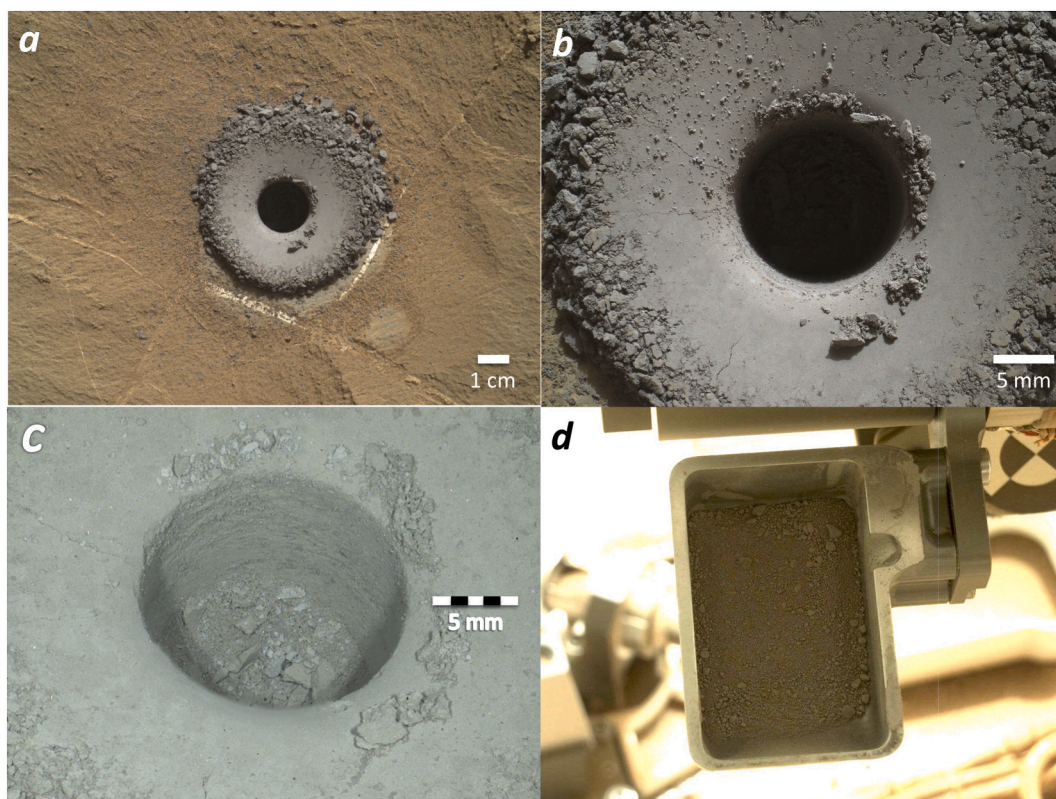


**Fig. 24.** Images from the Oudam full depth drill campaign. (a) MAHLI image of full depth drill hole taken at a standoff distance of 25 cm on Sol 1361 (1361MH0003970010502187C00). (b) MAHLI image of full depth drill hole taken at a standoff distance of 5 cm on Sol 1361 (1361MH0004230000502232R00). (c) MAHLI image of full depth drill hole taken from an oblique angle on Sol 1364 (1365MH0006210000502377R00). Image acquired at night under white light LED illumination. (d) Mastcam image of processed sample in scoop acquired on Sol 1362 using new scoop poses (1362ML0066650010600943E01). Note in all images drill hole is 1.6 cm in diameter. Scoop is 4.5 cm wide. *Image Credit:* NASA/JPL-Caltech/MSSS.

the team re-commenced full depth drilling on the Marimba target a few centimeters away from the initial attempt (Fig. 25). This time the Start Hole process was successful, taking 7 cycles to reach a depth of 4.88 mm using Percussion Levels 3 (cycles 1–4) and 4 (cycles 5–7) (Fig. 9a). The full drill penetrated the surface to a maximum total depth of 65.15 mm in 820 s total drill-on time with a cumulative average rate of penetration of 0.072 mm/s and a maximum Percussion Level of 4 (Figs. 9c & 12). On Sol 1423, however, transfer of the sample from the DBA to CHIMRA was aborted when multiple shorts were detected, likely caused by the percussion used during the transfer attempt. On Sol 1425 transfer was finally completed using vibration only (no percussion) and the sample was moved into the scoop where it was estimated that  $5.0 + 1.3/-0.3 \text{ cm}^3$  of material had been collected based on CAD models (Fig. 25d). The sample was then processed through the  $150 \mu\text{m}$  sieve path and portions were delivered to CheMin on the same sol. Subsequently, a portion was delivered to SAM on Sol 1443, with three additional portions delivered to SAM on Sol 1456. CheMin determined that Marimba has mineralogy similar to that of Oudam except with a much greater concentration of phyllosilicates ( $\sim 23 \text{ wt}\%$  vs  $\sim 3.3 \text{ wt}\%$  in Oudam) (Rampe et al., 2017b; Vaniman et al., 2018). Furthermore, using a combination of CheMin and SAM analyses, along with APXS measurements, it was determined that these clays are predominantly a mixture of Mg-rich trioctahedral and Al-rich dioctahedral smectites (Bristow et al., 2018), the first in situ detection of dioctahedral smectites on Mars. Previous phyllosilicates discovered by Curiosity, such as those at Yellowknife Bay, have been determined to be predominantly trioctahedral Fe-saponites (Bristow et al., 2015; Vaniman et al., 2014). The formation of Al-rich dioctahedral smectites from basaltic precursors requires greater elemental mobility than required for trioctahedral Fe-

bearing species, strongly suggesting that Marimba was subjected to more oxidizing conditions than samples collected lower down in the section. This is consistent with SAM measurements indicating much lower concentrations of carbon, nitrate, and (per)chlorate species in both Oudam and Marimba, also suggesting a major difference in diagenetic fluid composition (Stern et al., 2017; Sutter et al., 2017b).

#### 4.6.2. Quela

Quela was the seventh Murray mudstone target drilled. It is located about 32 m up section from Marimba. Since its bulk chemistry as determined by APXS and ChemCam is similar to previously drilled Murray targets and nearly identical to Marimba, it was decided that the team could proceed directly to full depth drilling. However, in order to potentially mitigate some of the problems encountered drilling at Marimba, it was also decided at the outset to allow the Start Hole procedure to be able to access Percussion Level 4. So, on Sol 1461, the team commenced with full depth drilling and caching of the Quela sample using the reduced percussion protocol. However, drilling was aborted when a short was detected, likely caused by percussion during the initiation of the Start Hole procedure (see above). On Sol 1464, after several sols of diagnostics, the team re-commenced with full depth drilling and caching of the Quela sample (Fig. 26). The Start Hole process took 5 cycles to reach a depth of 5.35 mm at Percussion Level 3 (Fig. 9a). The full drill penetrated the surface to a maximum total depth of 63.94 mm in 610 s total drill-on time with a cumulative average rate of penetration of 0.094 mm/s and a maximum Percussion Level of 3 (Figs. 9c & 12). On Sol 1465 the sample was transferred from the DBA to CHIMRA, using vibration only (no percussion), and into the scoop where it was estimated that  $6.1 + 1.3/-0.3 \text{ cm}^3$  of material had been collected

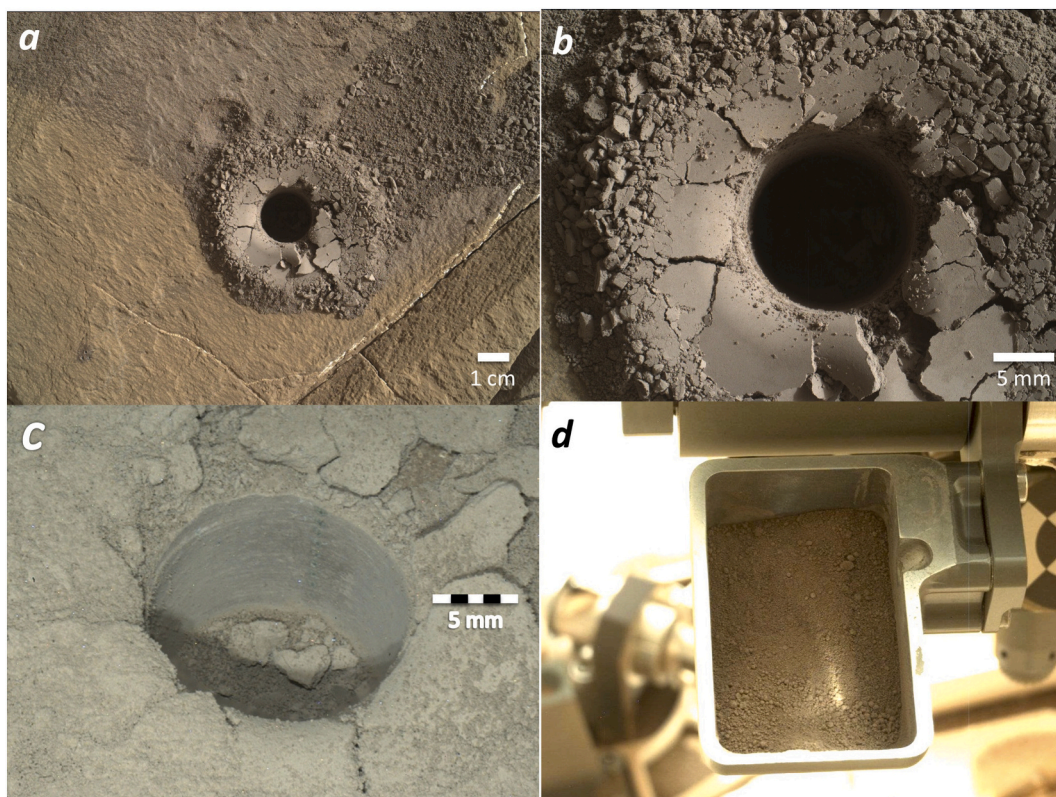


**Fig. 25.** Images from the Marimba full depth drill campaign. (a) MAHLI image of full depth drill hole taken at a standoff distance of 25 cm on Sol 1422 (1422MH0003970010503281C00). Note the aborted Start Hole from Sol 1420 to the upper left of the tailings pile. (b) MAHLI image of full depth drill hole taken at a standoff distance of 5 cm on Sol 1422 (1423MH0004230000503328R00). (c) MAHLI image of full depth drill hole taken from an oblique angle on Sol 1426 (1432MH0006310000503441R00). A vertical array of pits against the back wall of the can be seen created by the ChemCam laser. Image acquired at night under white light LED illumination. (d) Mastcam image of processed sample in scoop acquired on Sol 1425 (1425ML0070380010602387E01). Note in all images drill hole is 1.6 cm in diameter. Scoop is 4.5 cm wide. *Image Credit:* NASA/JPL-Caltech/MSSS.

based on CAD models (Fig. 26d). The sample was then processed through the 150  $\mu\text{m}$  sieve path and portions were delivered to CheMin on Sols 1466 and 1470. Subsequently, three portions were delivered to SAM on Sol 1484. CheMin and SAM results determined that Quela has mineralogy very similar to that of Marimba, including the presence of hematite and Al-rich dioctahedral smectites (Bristow et al., 2018; Rampe et al., 2017b).

#### 4.6.3. Sebina

Sebina was the eighth Murray mudstone target drilled. It is located 18–19 m up section from Quela. Since its bulk chemistry as determined by APXS and ChemCam is similar to previously drilled Murray samples, it was decided that the team could proceed directly to full depth drilling. However, the Start Hole procedure would begin at Percussion Level 1 this time, as was nominal for the reduced percussion protocol, but to avoid timing out before exceeding the minimum required depth of 4.5 mm, the procedure was altered so that the drill would automatically retry at Percussion Level 4 if needed, as it had been at Marimba. In addition, it had become routine while sampling the Murray formation to forgo either the mini-drill or mini-start hole test prior to drilling, which meant that no data had been gathered from the Hardness Test since Sol 1134 (Pilgrim). So it was decided to add the Hardness Test to the reduced percussion protocol going forward, however the level of percussion permitted would be capped at Level 4 (Step 6) to limit any further degradation of the drill system hardware. On Sol 1495 the team commenced with full depth drilling and caching of the Sebina sample using the reduced percussion protocol (Fig. 27). The Start Hole process took 7 cycles to reach a depth of 5.10 mm at Percussion Levels 1 (cycles

1–4) and 3 (cycles 5–7) (Fig. 9a). The Hardness Test increased the divot depth by 0.31 mm to a total of 5.41 mm (Fig. 9b). The full drill penetrated the surface to a maximum total depth of 65.38 mm in 680 s total drill-on time with a cumulative average rate of penetration of 0.087 mm/s and a maximum Percussion Level of 4 (Figs. 9c & 12). The sample was then transferred from the DBA to CHIMRA, using vibration only (no percussion), and into the scoop where it was estimated that  $6.3 + 1.3 / - 0.3 \text{ cm}^3$  of material had been collected based on CAD models (Fig. 27d). The sample was then processed through the 150  $\mu\text{m}$  sieve path and portions were delivered to CheMin on Sol 1496. No SAM analysis was performed on this sample. CheMin results determined that Sebina has mineralogy almost identical to that of both Marimba and Quela (Rampe et al., 2017b). The abundance of hematite and dioctahedral phyllosilicates in Oudam, Marimba, Quela, and Sebina, as well as the absence of magnetite, strongly suggests that the upper portion of the Murray formation was intensely altered by oxidizing fluids (Bristow et al., 2018; Rampe et al., 2017b). A paucity of mafic igneous minerals (e.g., pyroxene) in the upper Murray, when compared to mudstones lower in the section at Pahrump Hills and Yellowknife Bay, is also consistent with this interpretation.

## 5. Precipice and the drill feed fault

The rover's second unsuccessful drill attempt was made early in the third Martian year on a rock aptly dubbed 'Precipice'. If it had been successful, Precipice would have been the sixteenth rock drilled on Mars and the ninth full depth drill hole drilled into the Murray formation. It is located about 25 m up section from Sebina and would have been the fifth

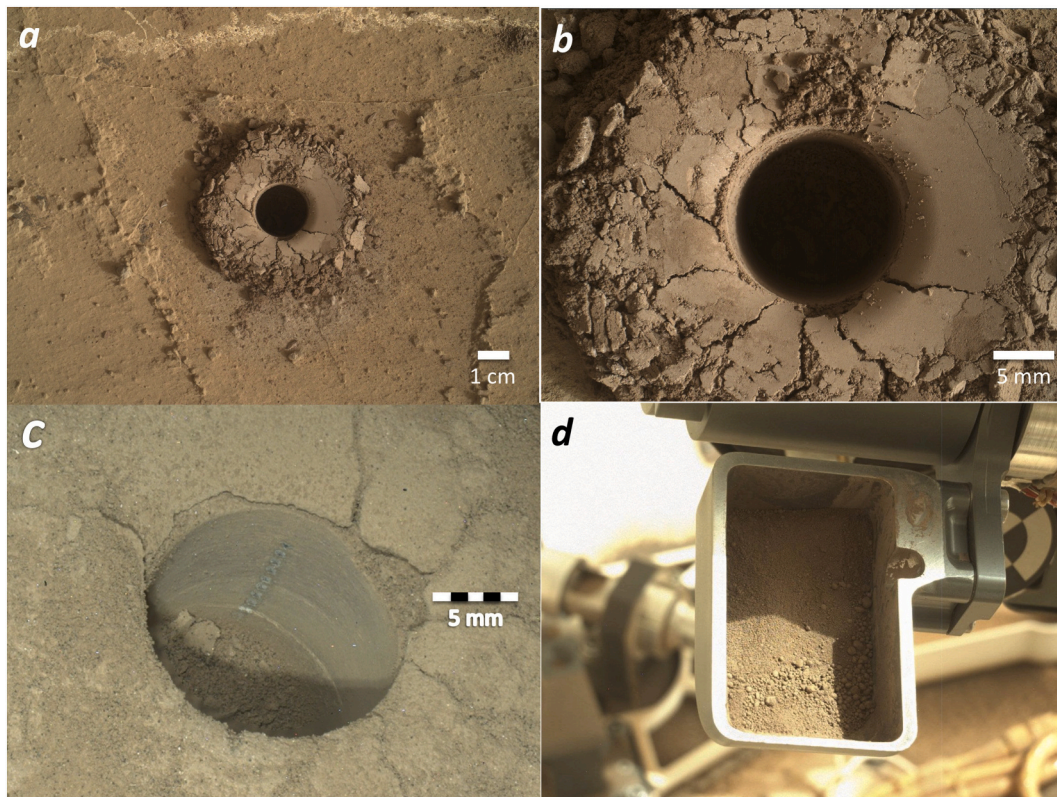


**Fig. 26.** Images from the Quela full depth drill campaign. (a) MAHLI image of full depth drill hole taken at a standoff distance of 25 cm on Sol 1464 (1464MH0003970010503887C00). (b) MAHLI image of full depth drill hole taken at a standoff distance of 5 cm on Sol 1464 (1465MH0004230000503932R00). (c) MAHLI image of full depth drill hole taken from an oblique angle on Sol 1472 (1472MH0006380000504073R00). A vertical array of pits against the back wall of the can be seen created by the ChemCam laser. Image acquired at night under white light LED illumination. (d) Mastcam image of processed sample in scoop acquired on Sol 1465 (1465ML0073260010603252E01). Note in all images drill hole is 1.6 cm in diameter. Scoop is 4.5 cm wide. *Image Credit:* NASA/JPL-Caltech/MSSS.

sample in the systematic stratigraphic survey of Murray mudstones being conducted as the rover progressed up Mt. Sharp. This also was the first attempt on Mars at using a non-percussive full depth drilling algorithm that relied solely on the rotation of the drill bit to penetrate a target. Given an increase in the number and severity of percussion-related faults that had been occurring over time, it was deemed necessary to determine if rotary-only drilling could be utilized in the event that percussion was no longer available. It should be noted that this was only a test and if it was unsuccessful, the plan was to still drill the target using the now standard reduced percussion protocol. In addition, since its bulk chemistry was similar to previously drilled Murray samples, it was decided that the team could proceed directly to full depth drilling without either a mini-drill or mini-start test hole. So, on Sol 1536 the team commenced with full depth drilling of the Precipice sample using the new non-percussion protocol. However, the drill attempt failed due to a stall in the drill feed mechanism, the motor that feeds the drill back and forth relative to the turret. This drill feed fault was unrelated to previous percussion-related faults. Given the seriousness of the fault and the time it would take before drilling could be safely resumed, the team decided to abandon Precipice without drilling. Diagnostics eventually determined that the drill would never operate as-designed again and subsequently the engineering team had to figure out a completely new way to continue drilling. The development of these work-arounds proceeded throughout the third Martian year and into the fourth before drilling was attempted again.

## 6. Conclusions and implications

During its second and third Martian years (Sols 669-2006) the MSL

rover successfully drilled twelve full depth drill holes on Mars and delivered sample to both the SAM and CheMin analytical laboratories onboard the rover. The first four drill holes, Confidence Hills (Sol 759), Mojave 2 (Sol 882), Telegraph Peak (908) and Buckskin (Sol 1060), were drilled into the Murray mudstones at the base of Mt. Sharp at Pahrump Hills and Marias Pass. The second four drill holes, Big Sky (Sol 1119), Greenhorn (Sol 1137), Lubango (Sol 1320) and Okoruso (Sol 1332), were drilled into the overlying Stimson sandstones at Bridger Basin and on the West Naukluft Plateau. The final four drill holes, Oudam (Sol 1361), Marimba (Sol 1422), Quela (Sol 1464) and Sebina (Sol 1495), were drilled into the Murray mudstones west of the Naukluft Plateau and in the Murray Buttes region on the drive toward Vera Rubin ridge. The unsuccessful attempt to drill a hole at Bonanza King (Sol 724) motivated the development and successful deployment of a new reduced percussion algorithm, starting with the Mojave 2 target. The reduced percussion algorithm improved the ability of the rover to interrogate weakly consolidated sedimentary materials going forward. However, repeated percussion related faults, starting on Sol 911, drove the development of an even newer non-percussion algorithm, first deployed on the Precipice target (Sol 1536). Unfortunately, this test was halted due to a drill feed fault, resulting in the end of drilling for the remainder of the third Martian year.

Together, the samples acquired over the course of this extended time period have demonstrated that Gale crater has experienced a rich and diverse aqueous past. Mudstones of the lower Murray formation appear to have been deposited in a lacustrine environment characterized by a complex pH/Eh history (Hurowitz et al., 2017; Rampe et al., 2017a). The mudstones of the upper Murray formation appear to have been intensely altered by diagenetic fluids more oxidizing than anything

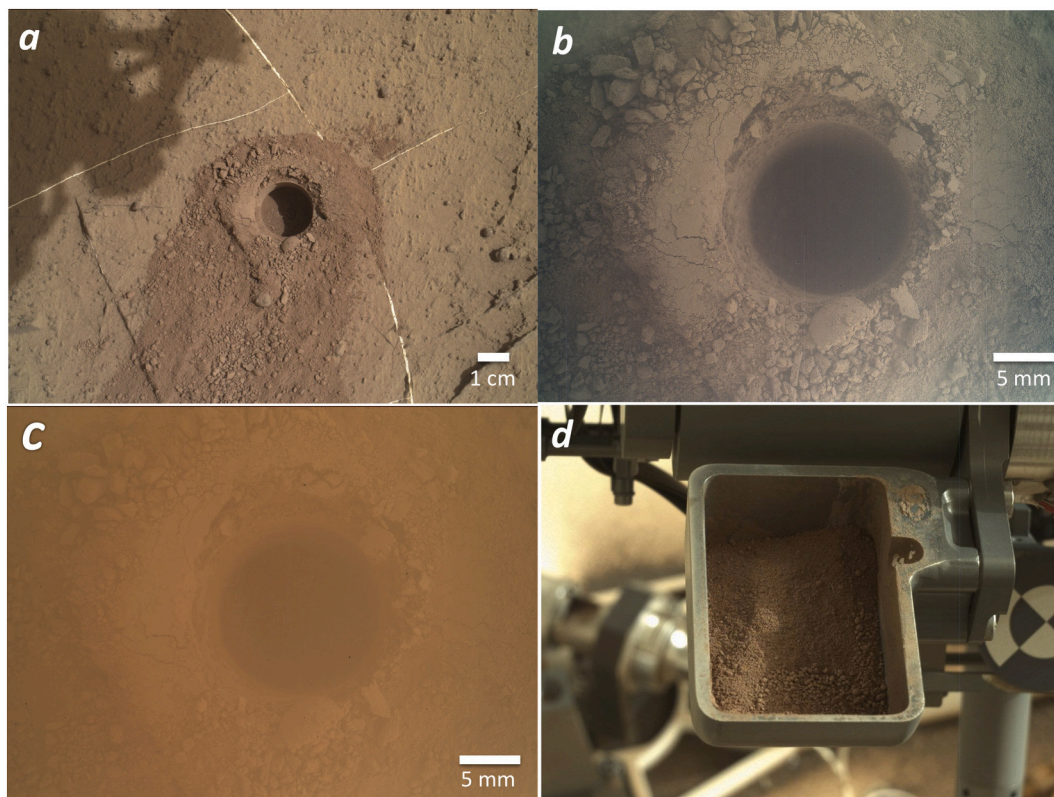


**Fig. 27.** Images from the Sebina full depth drill campaign. (a) MAHLI image of full depth drill hole taken at a standoff distance of 25 cm on Sol 1496 (1496MH0001900010504609C00). (b) MAHLI image of full depth drill hole taken at a standoff distance of 5 cm on Sol 1495 (1495MH0006400040504593C00). Note poor quality of image is due to acquisition through MAHLI lens cover, kept closed to keep out potential saltating grains, or drill fines mobilized by saltating grains, during a period of high seasonal winds. (c) For comparison, image of (b) prior to post-image processing. (d) Mastcam image of processed sample in scoop acquired on Sol 1495 (1495ML0075650010603868E01). Note in all images drill hole is 1.6 cm in diameter. Scoop is 4.5 cm wide. *Image Credit:* NASA/JPL-Caltech/MSSS.

experienced by either the lower Murray formation or the mudstones at Yellowknife Bay (Bristow et al., 2018; Rampe et al., 2017b; Sutter et al., 2017b). Meanwhile, the sandstones of the Stimson formation host fractures, some of the youngest features yet interrogated, that appear to be infiltrated by multiple stages of aqueous alteration, evolving over time from early acidic to late-stage neutral or alkaline fluids (Frydenvang et al., 2017; Hausrath et al., 2017; Yen et al., 2017). K-Ar dating of jarosite performed on the Mojave 2 sample yielded an upper age of  $\sim 4$  Ga for detrital minerals and a lower age of  $\sim 2$  Ga for local evaporite and/or phyllosilicate formation within the lower Murray mudstones (Martin et al., 2017). Also, well preserved organic material was discovered at Pahrump Hills (Confidence Hills and Mojave 2), despite the harsh surface conditions, suggesting even better preservation may be possible farther beneath the Martian surface (Eigenbrode et al., 2018). And finally, the first in situ identification of tridymite, gypsum, and dioctahedral smectite on the Martian surface occurred at Buckskin, Lubango, and Marimba, respectively (Bristow et al., 2018; Morris et al., 2016; Vaniman et al., 2017). The occurrence of tridymite is the first in situ mineralogic evidence for possible silicic magmatism on Mars. It should be noted that analysis of all of these samples is still on-going and one can expect that more will be revealed regarding the rich history of Mars with time.

#### Declaration of competing interest

The authors declare that they have no known competing financial interests or personal relationships that could have appeared to influence the work reported in this paper.

#### Acknowledgements

The work described in this paper was carried out at the Jet Propulsion Laboratory, California Institute of Technology, under a contract with the National Aeronautics and Space Administration. Funding was provided by the NASA Mars Science Laboratory Project (task order NNN13D846T). There were thousands of people who contributed to the Mars Science Laboratory project, overcoming challenges large and small on a daily basis, and we would like to thank the entire MSL team for the incredible dedication, ingenuity and perseverance that has enabled such a successful mission. The authors would also like to thank two anonymous reviewers whose comments greatly improved the quality of this manuscript. Finally, the authors would like to extend an extra special thank you to Dr. Joy Crisp for reviewing this manuscript and for all her years on MSL, helping us all do the best job we can, always with thoughtfulness and kind words.

#### References

- Abbey, W.J., Anderson, R., Beegle, L., Hurowitz, J., Williford, K., Peters, G., Morookian, J.M., et al., 2019. A look back: the drilling campaign of the Curiosity rover during the Mars Science Laboratory's Prime Mission. *Icarus* 319, 1–13. <https://doi.org/10.1016/j.icarus.2018.09.004>.
- Anderson, R.C., Jandura, L., Okon, A.B., Sunshine, D., Roumeliotis, C., Beegle, L.W., Hurowitz, J., Kennedy, B., Limonadi, D., McCloskey, S., Robinson, M., Seybold, C., Brown, K., 2012. Collecting samples in Gale crater, Mars: an overview of the Mars science laboratory sample acquisition, sample processing and handling system. *Space Sci. Rev.* 170, 57–75. <https://doi.org/10.1007/s11214-012-9898-9>.
- Banham, S.G., Gupta, S., Rubin, D.M., Watkins, J.A., Sumner, D.Y., Edgett, K.S., Grotzinger, J.P., et al., 2018. Ancient Martian aeolian processes and

- paleomorphology reconstructed from the Stimson formation on the lower slope of Aeolis Mons, Gale crater, Mars. *Sedimentology* 65, 993–1042.
- Bristow, T.F., Bish, D.L., Vaniman, D.T., Morris, R.V., Blake, D.F., Grotzinger, J.P., Rampe, E.B., et al., 2015. The origin and implications of clay minerals from Yellowknife Bay, Gale crater, Mars. *Am. Mineral.* 100, 824–836.
- Bristow, T.F., Rampe, E.B., Achilles, C.N., Blake, D.F., Chipera, S.J., Craig, P., Crisp, J.A., et al., 2018. Clay mineral diversity and abundance in sedimentary rocks of Gale crater, Mars. *Sci. Adv.* 4 (6), eaar3330. <https://doi.org/10.1126/sciadv.aar3330>.
- Cady, S.L., Farmer, J.D., Grotzinger, J.P., Schopf, J.W., Steele, A., 2003. Morphological biosignatures and the search for life on Mars. *Astrobiology* 3 (2), 351–368.
- Chairat, C., Schott, J., Oelkers, E.H., Lartigue, J.E., Harouiya, N., 2007. Kinetics and mechanism of natural fluorapatite dissolution at 25 °C and pH from 3 to 12. *Geochim. Cosmochim. Acta* 71, 5901–5912. <https://doi.org/10.1016/j.gca.2007.08.031>.
- Driscoll, R.L., Leinz, R.W., 2005. Methods for synthesis of some jarosites. In: *USGS Techniques and Methods 5-D1 (9 pp)*.
- Eigenbrode, J.L., Summons, R.E., Steele, A., Freissinet, C., Millan, M., Navarro-Gonzalez, R., Sutter, B., et al., 2018. Organic matter preserved in 3-billion-year-old mudstones at Gale crater, Mars. *Science* 360, 1096–1101. <https://doi.org/10.1126/science.aas9185>.
- Farley, K.A., Malespin, C., Mahaffy, P., Grotzinger, J.P., Vasconcelos, P.M., Milliken, R. E., Malin, M., et al., 2014. In situ radiometric and exposure age dating of the Martian surface. *Science* 343 (6169), 1247166. <https://doi.org/10.1126/science.1247166>.
- Fedo, C.M., Grotzinger, J.P., Gupta, S., Fraeman, A., Edgar, L., Edgett, K., Stein, N., et al., 2018. Sedimentology and stratigraphy of the Murray formation, Gale crater, Mars. In: *49th Lunar and Planetary Science Conference*, 19–23 March 2018.
- Fraeman, A.A., Edgar, L.A., Rampe, E.B., L'Haridon, J., Mangold, N., Thompson, L., Frydenvang, J., et al., 2020. The origin of Vera Rubin Ridge: Overview and results from Curiosity's exploration campaign. In: *51st Lunar and Planetary Science Conference*, 16–20 March 2020.
- Freissinet, C., Glavin, D.P., Mahaffy, P.R., Miller, K.E., Eigenbrode, J.L., Summons, R.E., Brunner, A.E., et al., 2015. Organic molecules in the sheepbed mudstone, Gale crater, Mars. *J. Geophys. Res. Planets* 120, 495–514. <https://doi.org/10.1002/2014JE004737>.
- Frydenvang, J., Gasda, P.J., Hurowitz, J.A., Grotzinger, J.P., Wiens, R.C., Newsom, H.E., Edgett, K.S., et al., 2017. Diagenetic silica enrichment and late-stage groundwater activity in Gale crater, Mars. *Geophys. Res. Lett.* 44, 4716–4724. <https://doi.org/10.1002/2017GL073323>.
- Grotzinger, J.P., Crisp, J., Vasavada, A.R., Anderson, R.C., Baker, C.J., Barry, R., Blake, D.F., et al., 2012. Mars science laboratory mission and science investigation. *Space Sci. Rev.* 170, 5–56. <https://doi.org/10.1007/s11214-012-9892-2>.
- Grotzinger, J.P., Sumner, D.Y., Kah, L.C., Stack, K., Gupta, S., Edgar, L., Rubin, D., et al., 2014. A habitable fluvio-lacustrine environment at Yellowknife Bay, Gale crater, Mars. *Science* 343 (6169). <https://doi.org/10.1126/science.1242777>.
- Grotzinger, J.P., Gupta, S., Malin, M.C., Rubin, D.M., Schieber, J., Siebach, K., Sumner, D.Y., et al., 2015. Deposition, exhumation, and paleoclimate of an ancient lake deposit, Gale crater, Mars. *Science* 350 (7575). <https://doi.org/10.1126/science.aac7575> PMID:26450214.
- Hausrath, E.M., Ming, D.W., Peretyazhko, T., Rampe, E.B., 2017. Using reactive transport modeling to understand formation of the Stimson sedimentary unit and altered fracture zones at Gale crater, Mars. In: *48th Lunar and Planetary Science Conference*, 20–24 March 2017.
- Helmick, D., McCloskey, S., Okon, A., Carsten, J., Kim, W., Leger, C., 2013. Mars science laboratory algorithms and flight software for autonomously drilling rocks. *J. Field Robot.* 30 (6), 847–874. <https://doi.org/10.1002/rob.21475>.
- Hurowitz, J., Grotzinger, J.P., Fischer, W.W., McLennan, S.M., Milliken, R.E., Stein, N., Vasavada, A.R., et al., 2017. Redox stratification of an ancient lake in Gale crater, Mars. *Science* 356, eaah6849. <https://doi.org/10.1126/science.aah6849>.
- Jandura, L., 2010. Mars science laboratory sample acquisition/sample processing and handling: subsystem design and test challenges. In: *Proceedings of the 40th Aerospace Mechanisms Symposium*.
- Kah, L.C., Stack, K.M., Eigenbrode, J.L., Yingst, R.A., Edgett, K.S., 2018. Syndepositional precipitation of calcium sulfate in Gale crater, Mars. *Terra Nova* 30 (6), 431–439. <https://doi.org/10.1111/ter.12359>.
- L'Haridon, J., Mangold, N., Meslin, P.-Y., Johnson, J.R., Rapin, W., Forni, O., Cousin, A., et al., 2018. Chemical variability in mineralized veins observed by ChemCam on the lower slopes of Mount Sharp in Gale crater, Mars. *Icarus* 311, 69–86. <https://doi.org/10.1016/j.icarus.2018.01.028>.
- Martin, P.E., Farley, K.A., Baker, M.B., Malespin, C.A., Schwenzer, S.P., Cohen, B.A., Mahaffy, P.R., McAdam, A.C., Ming, D.W., Vasconcelos, P.M., Navarro-Gonzalez, R., 2017. A two-step K-Ar experiment on Mars: dating the diagenetic formation of jarosite from Amazonian groundwaters. *J. Geophys. Res. Planets*. <https://doi.org/10.1002/2017JE005445>.
- Morris, R.V., Vaniman, D.T., Blake, D.F., Gellert, R., Chipera, S.J., Rampe, E.B., Ming, D. W., et al., 2016. Silicic volcanism on Mars evidenced by tridymite in high-SiO<sub>2</sub> sedimentary rock on Gale crater. *PNAS* 113 (26), 7071–7076. [www.pnas.org/cgi/doi/10.1073/pnas.1607098113](http://www.pnas.org/cgi/doi/10.1073/pnas.1607098113).
- Nachon, M., Mangold, N., Forni, O., Kah, L.C., Cousin, A., Wiens, R.C., Anderson, R.B., et al., 2017. Chemistry of diagenetic features analyzed by ChemCam at Pahrump Hills, Gale crater, Mars. *Icarus* 281, 121–136. <https://doi.org/10.1016/j.icarus.2016.08.026>.
- Okun, A., 2010. Mars science laboratory drill. In: *Proceedings of the 40th Aerospace Mechanisms Symposium*.
- Peters, G.H., Carey, E.M., Anderson, R.C., Abbey, W.J., Kinnert, R., Watkins, J.A., Schemel, M., et al., 2018. Uniaxial compressive strengths of rocks drilled at Gale crater, Mars. *Geophys. Res. Lett.* 45, 108–116. <https://doi.org/10.1002/2017GL075965>.
- Rampe, E.B., Ming, D.W., Blake, D.F., Bristow, T.F., Chipera, S.J., Grotzinger, J.P., Morris, R.V., et al., 2017a. Mineralogy of an ancient lacustrine mudstone succession from the Murray formation, Gale crater, Mars. *Earth Planet. Sci. Lett.* 471, 172–185. <https://doi.org/10.1016/j.epsl.2017.04.021>.
- Rampe, E.B., Ming, D.W., Grotzinger, J.P., Morris, R.V., Blake, D.F., Vaniman, D.T., Bristow, T.F., et al., 2017b. Mineral trends in early Hesperian lacustrine mudstone at Gale crater, Mars. In: *48th Lunar and Planetary Science Conference*, 20–24 March 2017.
- Smith, D.E., Zuber, M.T., Frey, H.V., Garvin, J.B., Head, J.W., Muhleman, D.O., Pettengill, G.H., et al., 2001. Mars orbiter laser altimeter: experiment summary after the first year of global mapping of Mars. *J. Geophys. Res.* 106, 23689–23722. <https://doi.org/10.1029/2000JE001364>.
- Stack, K.M., Cofield, S.M., Fraeman, A.A., 2017. Geologic map of the MSL curiosity rover extended mission traverse of Aeolis Mons, Gale crater, Mars. In: *48th Lunar and Planetary Science Conference*, 20–24 March 2017.
- Stern, J.C., Sutter, B., Jackson, W.A., Navarro-Gonzalez, R., McKay, C.P., Ming, D.W., Archer, P.D., Mahaffy, P.R., 2017. The nitrate/(per)chlorate relationship on Mars. *Geophys. Res. Lett.* 44, 2643–2651. <https://doi.org/10.1002/2016GL072199>.
- Sunshine, D., 2010. Mars science laboratory CHIMRA: a device for processing powdered Martian samples. In: *Proceedings of the 40th Aerospace Mechanisms Symposium*.
- Sutter, B., McAdam, A.C., Mahaffy, P.R., Ming, D.W., Edgett, K.S., Rampe, E.B., Eigenbrode, J.L., et al., 2017a. Evolved gas analyses of sedimentary rocks and eolian sediment in Gale crater, Mars: results of the Curiosity rover's sample analysis at Mars instrument from Yellowknife Bay to the Namib Dune. *J. Geophys. Res. Planets* 122. <https://doi.org/10.1002/2016JE005225>.
- Sutter, B., McAdam, A.C., Rampe, E.B., Thompson, L.M., Ming, D.W., Mahaffy, P.R., Navarro-Gonzalez, R., Stern, J.C., Eigenbrode, J.L., Archer, P.D., 2017b. Evolved gas analyses of the Murray formation in Gale crater, Mars: results of the Curiosity rover's sample analysis at Mars (SAM) instrument. In: *48th Lunar and Planetary Science Conference*, 20–24 March 2017.
- Thompson, L.M., Schmidt, M.E., Gellert, R., Spray, J.G., the MSL APXS Team, 2016. APXS compositional trends along Curiosity's traverse, Gale crater, Mars: implications for crustal composition, sedimentary provenance, diagenesis and alteration. In: *47th Lunar and Planetary Science Conference*, 21–25 March, 2016.
- Treiman, A.H., Bish, D.L., Vaniman, D.T., Chipera, S.J., Blake, D.F., Ming, D.W., Morris, R.V., et al., 2016. Mineralogy, provenance, and diagenesis of a potassic basaltic sandstone on Mars: ChemMin X-ray diffraction of the Windjana sample (Kimberley area, Gale Crater). *J. Geophys. Res. Planets* 121 (1), 75–106. <https://doi.org/10.1002/2015JE004932>.
- Vaniman, D.T., Bish, D.L., Ming, D.W., Bristow, T.F., Morris, R.V., Blake, D.F., Chipera, S. J., et al., 2014. Mineralogy of a mudstone at Yellowknife Bay, Gale crater. *Mar. Sci.* 343, 1243480.
- Vaniman, D.T., Martinez, G.M., Rampe, E.B., Bristow, T.F., Blake, D.F., Yen, A.H., Ming, D.W., Rapin, W., Meslin, P.-Y., Morookian, J.M., 2017. Calcium sulfates at Gale crater and limitations on gypsum stability. In: *48th Lunar and Planetary Science Conference*, 20–24 March 2017.
- Vaniman, D.T., Martinez, G.M., Rampe, E.B., Bristow, T.F., Blake, D.F., Yen, A.H., Ming, D.W., et al., 2018. Gypsum, bassanite, and anhydrite at Gale crater, Mars. *Am. Mineral.* 103, 1011–1020. <https://doi.org/10.2138/am-2018-6346>.
- Vasconcelos, P.M., Farley, K.A., Malespin, C.A., Mahaffy, P., Ming, D., McLennan, S.M., Hurowitz, J.A., Rice, S.M., 2016. Discordant K-Ar and young exposure dates for the Windjana sandstone, Kimberley, Gale crater, Mars. *J. Geophys. Res. Planets* 121, 2176–2192. <https://doi.org/10.1002/2016JE005017>.
- Wiens, R.C., Mangold, N., Maurice, S., Gasnault, O., Clegg, S., Blaney, D., Gasda, P., et al., 2016. Major-element composition seen by ChemCam along the curiosity rover traverse: the first 8,000 observations. In: *47th Lunar and Planetary Science Conference*, 21–25 March, 2016.
- Yen, A.S., Ming, D.W., Vaniman, D.T., Gellert, R., Blake, D.F., Morris, R.V., Morrison, S. M., et al., 2017. Multiple stages of aqueous alteration along fractures in mudstones and sandstone strata in Gale crater, Mars. *Earth Planet. Sci. Lett.* 471, 186–198. <https://doi.org/10.1016/j.epsl.2017.04.033>.